Volcanism, Structure, and Geochronology of Long Valley Caldera, Mono County, California

ROY A. BAILEY

U.S. Geological Survey, Reston, Virginia 22092

G. BRENT DALRYMPLE AND MARVIN A. LANPHERE

U.S. Geological Survey, Menlo Park, California 94025

Long Valley caldera, a 17- by 32-km elliptical depression on the east front of the Sierra Nevada, formed 0.7 m.y. ago during eruption of the Bishop tuff. Subsequent intracaldera volcanism included eruption of (1) aphyric rhyolite 0.68–0.64 m.y. ago during resurgent doming of the caldera floor, (2) porphyritic hornblende-biotite rhyolite from centers peripheral to the resurgent dome at 0.5, 0.3, and 0.1 m.y. ago, and (3) porphyritic hornblende-biotite rhyodacite from outer ring fractures 0.2 m.y. ago to 50,000 yr ago, a sequence that apparently records progressive crystallization of a subjacent chemically zoned magma chamber. Holocene rhyolitic and phreatic eruptions suggest that residual magma was present in the chamber as recently as 450 yr ago. Intracaldera hydrothermal activity began at least 0.3 m.y. ago and was widespread in the caldera moat; it has since declined due to self-sealing of near-surface caldera sediments by zeolitization, argillization, and silicification and has become localized on recently reactivated northwest-trending Sierra Nevada frontal faults that tap hot water at depth.

INTRODUCTION

In the western United States, only three calderas are known to be large enough and young enough to possibly still contain residual magma in their chambers: the Valles caldera (~1.1 m.y. old) in north central New Mexico; the Long Valley caldera (~0.7 m.y. old) in central eastern California, and the Yellowstone caldera (~0.6 m.y. old) in northwestern Wyoming. Detailed mapping of the Valles caldera [*Smith et al.*, 1961, 1970] and the Yellowstone caldera [*Christiansen and Blank*, 1969; *U.S. Geological Survey*, 1972; *Keefer*, 1972] has contributed much to the understanding of caldera evolution and mechanisms. Long Valley caldera (Figures 1 and 2) heretofore has not been mapped in detail, although a number of excellent studies of the general geology of the region have been made, notably by *Gilbert* [1938, 1941], *Gilbert et al.* [1968], *Kistler* [1966*a*, *b*], *Rinehart and Ross* [1957, 1964], and *Huber and Rinehart* [1967]. Inclusion of Long Valley as one of the target areas of the U.S. Geological Survey Geothermal Research Program has provided an opportunity to apply a wide range of geologic, geochemical, and geophysical techniques to the study of a large, active geothermal system; it also has provided the first opportunity to synthesize the volcanic history of this fascinating area. This paper is a preliminary report of the geologic and chronological studies based on mapping and sampling carried on during the summers of 1972 and 1973. Geologic mapping and petrologic studies are continuing. The petrologic model presented in the summary is based primarily on field studies, supplemented by preliminary petrography and limited preexisting petrochemical data, and should be considered tentative.

K-AR DATING TECHNIQUE

Samples for age measurement were collected from outcrops at locations shown on Figure 3. When it was possible, biotite or sanidine in the size range of 149–420 μm was separated by using standard magnetic and heavy liquid techniques. Sanidine concentrates were treated with a dilute HF solution to remove small bits of attached glass and fragments of other mineral grains. Obsidian used for dating was totally unhydrated and not devitrified. Small blocks sawed from many of the hand specimens were used for dating. For samples that contained phenocrysts the obsidian was crushed to between 2 and 4 mm, and pure glass fragments were handpicked for analysis. Basalt and andesite were examined in thin sections to be sure that they met the usual criteria for whole-rock K-Ar dating [*Mankinen and Dalrymple*, 1972].

Argon was measured by isotope dilution mass spectrometry using an ^{38}Ar tracer and extraction techniques, mass analysis, and data reduction procedures described by *Dalrymple and Lanphere* [1969]. Potassium was determined by using the lithium metaborate fusion technique and flame photometry [*Suhr and Ingamells*, 1966; *Ingamells*, 1970]. Errors given in Table 1 and in the text are standard deviations of analytical precision, estimated by using the method of *Cox and Dalrymple* [1967].

The analytical data and calculated K-Ar ages are given in Table 1 and discussed in the appropriate sections along with the stratigraphy, petrology, and structure. A summary of the age data, showing stratigraphic relations and relevant statistical data, is presented in Figure 4.

GEOLOGIC SETTING

Long Valley caldera is at the east base of the Sierra Nevada, 50 km northwest of the town of Bishop and 30 km south of Mono Lake (Figure 1). The caldera is an elliptical depression about 32 km from east to west by 17 km from north to south; it has an area of about 450 km² (Figure 2). The eastern half of the caldera, Long Valley proper, is a broad, crescentic grass- and sage-covered valley of low relief, at an elevation near 2070 m (6800 ft). The western half of the caldera is a forested area of higher relief at an average elevation of 2440 m (8000 ft); it forms the 'Mammoth embayment,' a prominent reentrant in the Sierra Nevada range front near the town of Mammoth Lakes. In the west central part of the caldera a group of faulted and dissected hills rises to 2590-m (8500 ft) elevation. Between

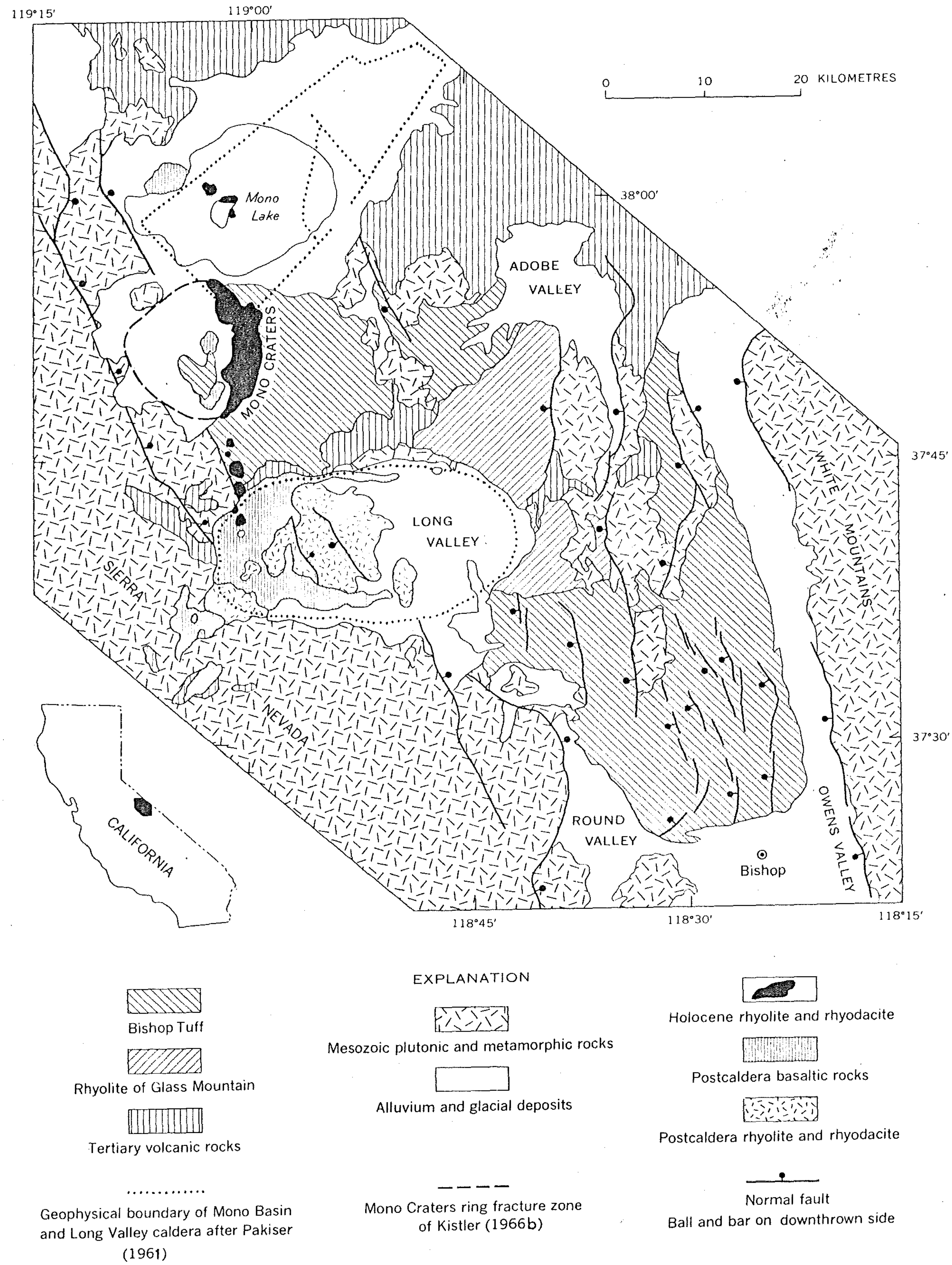

Fig. 1. Index map and generalized geologic map of the Long Valley–Mono basin area.

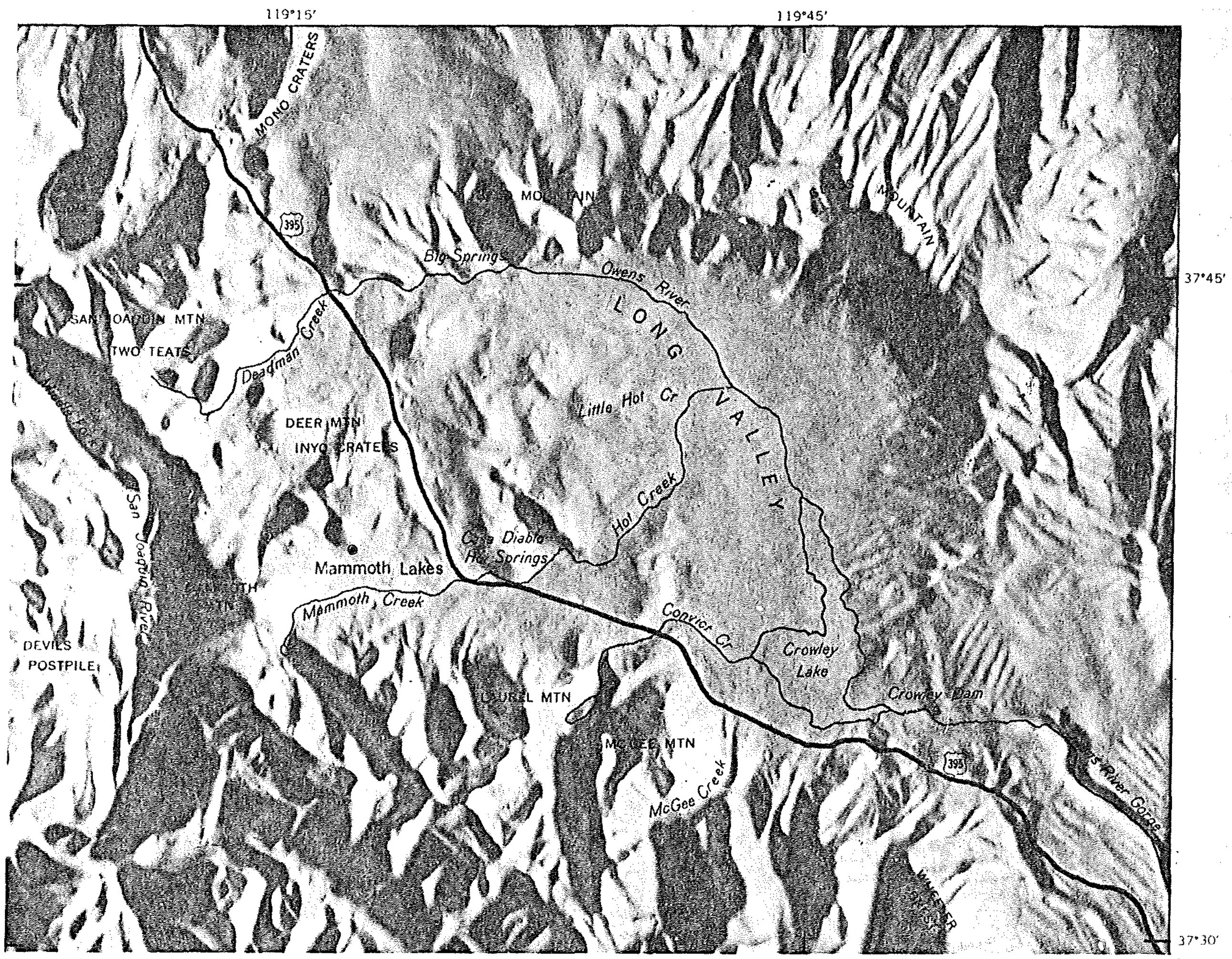

Fig. 2. Shaded relief map of Long Valley caldera.

these central hills and the caldera walls is an annular moat, which is drained on the north by Deadman Creek and the upper Owens River and on the south by Mammoth Creek and Hot Creek. The walls of the caldera are well defined and rise steeply on all sides except the southeast. On the south the wall rises precipitously 1000 m to remnants of a late Tertiary erosion surface [*Rinehart and Ross*, 1964, Plate 1; *Curry*, 1971] at an elevation of 3050 m (10,000 ft) on the shoulders of McGee and Laurel mountains. In the west the wall rises 500 m to the eastern slopes of San Joaquin Mountain and Two Teats. On the north and northeast the wall is formed by the steep south face of Bald Mountain and of Glass Mountain, which rises 1200 m to an elevation of about 3350 m (11,000 ft). The east wall, in contrast, is a low terraced escarpment with a maximum relief of only 250 m, and the southeast wall is little more than an arch that merges with the surface of the Volcanic Tableland, which slopes gently southeast toward Bishop.

The pre-Tertiary basement rocks in the immediate vicinity of Long Valley caldera are Jurassic and Cretaceous granodiorites and granites of the Sierra Nevada batholith and Paleozoic and Mesozoic metamorphic rocks of the Mount Morrison and Ritter range roof pendants [*Bateman et al.*, 1963; *Rinehart and Ross*, 1964] (Figure 3). Overlying the basement rocks on an erosion surface of moderate relief are late Tertiary volcanic rocks, mainly basalt, andesite, and rhyodacite.

Basalt and andesite flows with a cumulative thickness of 200–250 m crop out in the west wall of the caldera, as well as along part of the north wall. Thinner, less extensive sequences of flows from small local centers occur also on the east rim south of Glass Mountain and on the south rim on McGee Mountain. Rhyodacites overlie the basaltic rocks on the west rim and form the main mass of San Joaquin Mountain and Two Teats, the dissected remnants of a large Pliocene volcano northwest of the caldera. Three additional masses of rhyodacite, the largest of which is Bald Mountain, occur on the north rim.

Abundant basaltic inclusions found in postsubsidence intracaldera rhyolites suggest that the thick sequences of basaltic rocks on the west and north walls extend well into the caldera area. In contrast, rhyodacite inclusions are rare in the postcaldera rhyolites, suggesting that no comparable thickness of rhyodacite occurs within the caldera. The available evidence indicates that no great accumulation or edifice of precaldera volcanic rocks existed within the caldera area, as is true of many other resurgent cauldrons [*Smith and Bailey*, 1968; *Smith et al.*, 1970]. The wide and sporadic distribution of precaldera volcanic centers suggests that these Tertiary rocks are not directly related to the Long Valley magma chamber, although they may represent an early part of the volcanic cycle that culminated with the voluminous rhyolites of Long Valley.

These Tertiary volcanic rocks range in age from 3.2 to 2.6 m.y. old. Units in the vicinity of Long Valley that have been dated by the K-Ar method include (1) the basalt at Old Mam-

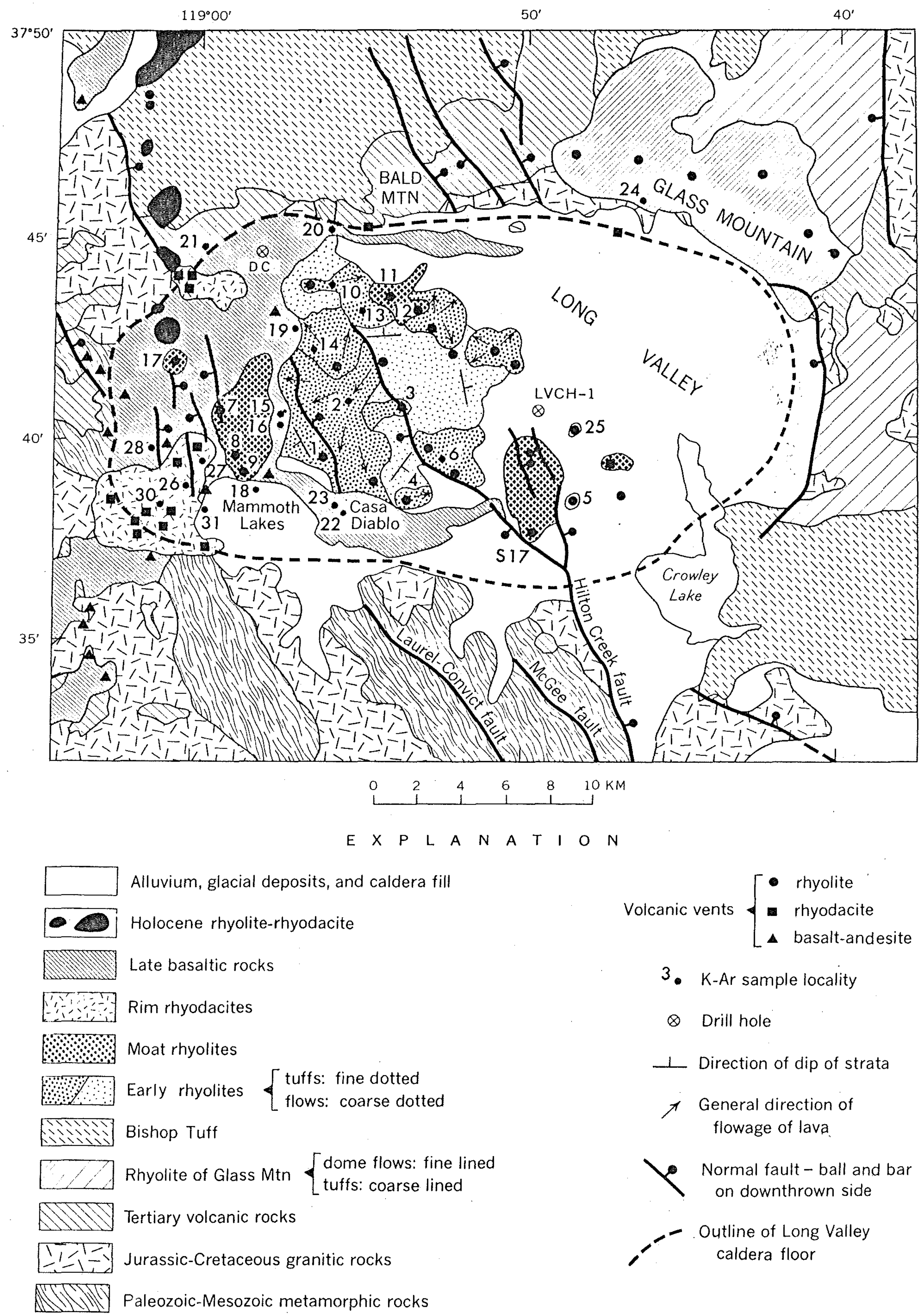

Fig. 3. Generalized geologic map of Long Valley caldera.

TABLE 1. K-Ar Age Data on Volcanic Rocks From Long Valley Caldera, California

Sample No.	Map No. (Figure 3)	Rock Type	Material Dated	K_2O*, wt %	Argon: Weight, g	Argon: $^{40}Ar_{rad}$, 10^{-12}mol/g	Argon: $100\,^{40}Ar_{rad}/^{40}Ar_{total}$	Calculated Age,† 10^6 yr
72G001	1	Aphyric rhyolite	Obsidian	5.10 (2)	3.470	5.189	43.5	0.675 ± 0.016
					3.461	4.948	29.1	
72G002	2	Biotite rhyolite	Obsidian	5.24 (2)	4.228	5.125	53.4	0.660 ± 0.027
					4.188	5.070	16.5	
72G003	3	Pyroxene rhyolite	Obsidian	5.25 ± 0.06 (4)	3.870	5.199	16.7	0.664 ± 0.029
					4.075	5.131	34.6	
72G004	4	Pyroxene rhyolite	Obsidian	5.22 (2)	4.426	5.312	34.7	0.670 ± 0.014
					4.442	5.057	57.0	
72G005	5	Hornblende-biotite rhyolite	Sanidine	10.96 (2)	5.828	5.263	48.2	0.324 ± 0.010
72G006	6	Pyroxene rhyolite	Obsidian	5.02 (2)	4.089	5.583	46.4	0.73 ± 0.016
					4.197	5.280	45.3	
72G007	7	Hornblende-biotite rhyolite	Sanidine	10.88 (2)	12.182	1.724	64.4	0.106 ± 0.003
72G008	8	Hornblende-biotite rhyolite	Sanidine	11.24 (2)	5.080	1.330	9.1	0.094 ± 0.006
					5.872	1.590	33.5	
72G009	9	Hornblende-biotite rhyolite	Sanidine	11.32 (2)	6.755	1.735	38.8	0.103 ± 0.002
					6.112	1.744	34.2	
72G010	10	Aphyric rhyolite	Obsidian	5.07 (2)	3.430	5.145	43.9	0.673 ± 0.014
					4.458	4.967	53.0	
72G011	11	Hornblende-biotite rhyolite	Sanidine	10.64 (2)	6.544	7.293	40.4	0.468 ± 0.010
					7.160	7.440	40.7	
72G012	12	Hornblende-biotite rhyolite	Sanidine	10.45 (2)	5.799	8.023	62.3	0.509 ± 0.011
					5.158	7.730	76.0	
72G013	13	Aphyric rhyolite	Obsidian	5.14 (2)	4.932	4.992	54.5	0.658 ± 0.014
					5.384	5.036	41.6	
72G014	14	Pyroxene rhyolite	Obsidian	5.15 (2)	3.955	4.958	57.4	0.634 ± 0.013
					3.908	4.725	34.5	
72G015	15	Basalt	Whole-rock	1.654 (2)	10.578	0.367	3.1	0.149 ± 0.070
72G016	16	Basalt	Whole-rock	1.663 (2)	11.078	0.372	8.8	0.151 ± 0.027
72G017	17	Hornblende-biotite rhyolite	Sanidine	10.63 (2)	4.347	1.890	24.8	0.113 ± 0.004
					12.901	1.728	32.2	
73G001	18	Andesite	Whole-rock	2.13 ± 0.01 (4)	9.102	0.700	2.8	0.222 ± 0.080
73G008	19	Basalt	Whole-rock	2.00 ± 0.00 (4)	8.379	0.428	8.8	0.145 ± 0.015
73G009	20	Basalt	Whole-rock	1.63 ± 0.05 (8)	12.256	0.271	13.3	0.104 ± 0.011
					14.187	0.201	4.3	
73G010	21	Andesite	Whole-rock	3.01 ± 0.01 (4)	14.401	12.787	70.2	2.87 ± 0.09
73G012	22	Basalt	Whole-rock	2.26 ± 0.06 (4)	5.837	0.482	5.5	0.126 ± 0.025
					7.784	0.372	4.7	
73G014	23	Basalt	Whole-rock	1.82 ± 0.01 (4)	12.806	0.148	4.3	0.062 ± 0.013
					11.736	0.194	3.5	
73G016	24	Biotite rhyolite	Sanidine	9.75 ± 0.26 (4)	1.053	27.749	61.6	1.92 ± 0.05
73G017	25	Hornblende-biotite rhyolite	Sanidine	11.34 ± 0.03 (4)	4.084	6.029	55.5	0.349 ± 0.006
					3.433	5.812	58.2	
			Biotite	8.93 ± 0.06 (4)	1.337	6.645	4.7	0.503 ± 0.105
73G018	26	Rhyodacite	Biotite	8.60 (2)	1.688	2.212	4.1	0.145 ± 0.029
					1.995	1.422	2.8	
73G019	27	Rhyodacite	Biotite	7.12 (2)	1.897	1.460	2.6	0.138 ± 0.079
73G021	28	Basalt	Whole-rock	1.57 ± 0.01 (4)	11.928	0.211	5.7	0.093 ± 0.012
					10.930	0.225	4.8	
73G023	29	Rhyodacite	Sanidine	7.76 (2)	2.251	0.582	9.2	0.050 ± 0.010
73G024	30	Rhyodacite	Biotite	8.22 (2)	1.841	1.436	2.4	0.118 ± 0.048
73G025	31	Andesite	Whole-rock	2.63 ± 0.01 (4)	7.543	0.366	7.1	0.083 ± 0.010
					9.418	0.320	14.8	

*Mean and, where more than two measurements were made, standard deviation. Number of measurements is in parentheses.

†$\lambda_\epsilon = 0.585 \times 10^{-10}$ yr^{-1}, $\lambda_\beta = 4.72 \times 10^{-10}$ yr^{-1}, $^{40}K/K = 1.19 \times 10^{-4}$ mol/mol. Where more than one measurement was made on a sample, the age given is the weighted mean; weighting was by the inverse of the variance. Errors given are estimates of the standard deviation of analytical precision [*Cox and Dalrymple*, 1967].

moth Mine and (2) andesite from San Joaquin ridge, both 3.1 ± 0.1 m.y. old [*Dalrymple*, 1964*a*]; (3) basalts in the Benton range that erupted from a cone on the northeast rim of the caldera 3.2 ± 0.1 m.y. ago [*Dalrymple*, 1964*a*]; (4) basalt in the Owens River gorge, 3.2 ± 0.1 m.y. old [*Dalrymple*, 1963]; (5) andesite in the northwest wall, 2.87 ± 0.09 m.y. old (location 10; location numbers refer to map locations in Figure 3 and Table 1); (6) basalt on McGee Mountain, 2.6 ± 0.1 m.y. old [*Dalrymple*, 1963]; and (7) quartz latites from Two Teats, 3.0 ± 0.1 m.y. old [*Dalrymple*, 1964*a*] and 2.7 ± 0.1 m.y. old [*Curry*, 1966].

RHYOLITES OF GLASS MOUNTAIN

The earliest volcanic rocks that can be related to the Long Valley magma chamber are the rhyolites of Glass Mountain (Figure 3). Glass Mountain is a thick accumulation (>1000 m) of domes, flows, and shallow intrusions flanked by extensive fans of pyroclastic deposits that consist of pumice and ash

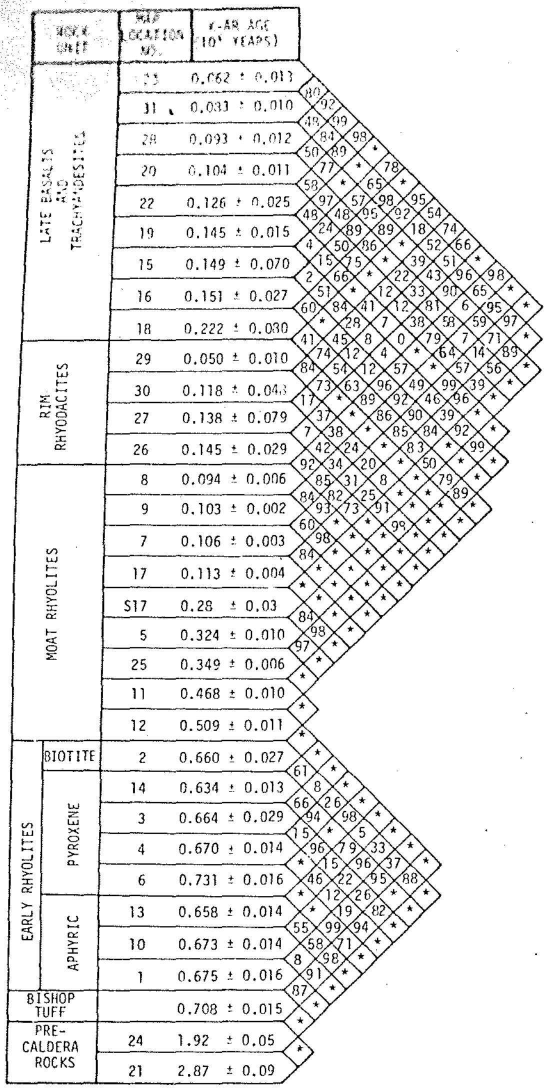

Fig. 4. Maximum probability, in percent, that the calculated ages of any two volcanic units are truly different and not the result of random errors in the analytical procedure. A probability of more than 99% is indicated by an asterisk.

falls, small ash flows, blocky Pelean avalanche deposits, and epiclastic conglomeratic sediments [*Gilbert*, 1941; *Rinehart and Ross*, 1957]. Dissected remnants of the flanking fans extend northeast into Adobe Valley and south along the east side of the caldera. Similar fans probably extended southwest from Glass Mountain, but the southwest half of the mountain has been downfaulted along the caldera boundary faults and is now buried beneath the sedimentary and volcanic fill of Long Valley. The vents and intrusive centers of Glass Mountain are well exposed in its south face. They are arranged in an arc approximately parallel to the northeast wall of Long Valley caldera, which suggests that their location was controlled by an incipient caldera ring fracture and that they represent early leakage from the Long Valley magma chamber.

The rhyolites of Glass Mountain are aphyric to sparsely porphyritic, and, according to *Noble et al.* [1972], are highly differentiated, peraluminous, and high in silica (containing about 77%). Two K-Ar ages, one of 0.90 ± 0.10 m.y. obtained on sanidine from obsidian near the top of Glass Mountain [*Gilbert et al.*, 1968, p. 302] and another of 1.92 ± 0.05 m.y. on sanidine from a biotite rhyolite low on the southwest side (location 16), indicate that Glass Mountain was built by eruptions that extended over a period of at least 1 m.y.

BISHOP TUFF

The Bishop tuff, a voluminous rhyolite ash flow sheet, erupted about 0.7 m.y. ago [*Dalrymple et al.*, 1965] from vents now buried within Long Valley caldera [*Gilbert*, 1938, pp. 1859–1860]. From these vents, ash flows spread radially southeast through the low area now occupied by the Owens River, north over the west shoulder of Glass Mountain into Adobe Valley, northwest over Deadman Summit into Mono basin, and west over the low pass now occupied by Mammoth Mountain into the valley of the Middle Fork of the San Joaquin River (Figure 1). The most extensive exposure of Bishop tuff is on the Volcanic Tableland southeast of the caldera [*Gilbert*, 1938; *Sheridan*, 1965]. Lesser exposures occur in the southeastern part of the Adobe Valley and in the southern part of the Mono basin [*Gilbert*, 1938], where the sheet is extensively covered by pumice from the Mono craters. Small erosional remnants also cling to the walls of the Middle Fork of the San Joaquin near Reds Meadow [*Huber and Rinehart*, 1967].

The Bishop tuff is a crystal-rich rhyolite tuff that contains up to 30% phenocrysts of quartz, sanidine, plagioclase, biotite, and Fe-Ti oxides [*Gilbert*, 1938; *Sheridan*, 1965]. Available chemical data [*Bateman*, 1965, Table 21; *Sheridan*, 1965, Table 5] indicate that the Bishop tuff differs only slightly in composition from top to bottom and is not a strongly differentiated sheet. According to *Sheridan* [1968] the tuff exposed in the lower Owens River gorge is a double cooling unit, which indicates that it was emplaced during two eruptive pulses.

Gilbert [1938, p. 1833] estimated that the Bishop tuff covers an area of 1040–1150 km² and has a volume of about 140 km³. His estimate, however, did not include the large volume of tuff buried within the caldera. Although Bishop tuff is not exposed anywhere within the caldera, blocks of the tuff occur as accidental inclusions in early postcaldera rhyolite tuffs exposed in the central part of the caldera, clearly indicating that Bishop tuff underlies the tuffs at depth [*Bailey*, 1973]. Most of the inclusions are of densely welded tuff, suggesting that the intracaldera Bishop tuff is probably quite thick. By analogy with intracaldera welded tuffs exposed in older, more deeply dissected resurgent cauldrons [*Ratté and Steven*, 1967; *Byers et al.*, 1968; *Lipman and Steven*, 1970; *Lipman et al.*, 1973; R. L. Smith and R. A. Bailey, unpublished data, 1970], the intracaldera Bishop tuff is probably of the order of 1000 m thick. Seismic refraction studies of the caldera [*Hill*, 1976] suggest a thickness of 1000–1500 m. By using a thickness of 1000 m and the area of the subsided cauldron block (350 km² as defined by the inferred position of the main boundary faults in the caldera moat), the volume of intracaldera Bishop tuff is estimated to be about 350 km³. Thus the total volume of Bishop ash flows is of the order of 500 km³, two-thirds of which accumulated within the subsiding caldera.

The volume of Bishop ash that was carried away by winds and thinly dispersed over much of the western United States is difficult to estimate on the basis of presently available data. However, using (1) the distribution of Bishop ash indicated by *Izett et al.* [1970] and (2) one-half the maximum thickness (3 m) of Bishop pumice fall in the vicinity of the caldera and (3) assuming logarithmic thinning of the ash downwind, we calculate a volume of 300 km³. Although this estimate seems surprisingly large, we believe our method of calculation yields a conservative figure. Furthermore, the relative proportion of ash fall to ash flows (3:5) does not seem unreasonable when it is compared with the ratio (1:1) of the Mazama ash to its associated Crater Lake ash flows [*Williams and Goles*, 1968], especially when one takes into account the likelihood that the Crater Lake eruption had a stronger vertical component.

The foregoing volumes of ash and tuff, when they are reduced by appropriate factors for their porosity, indicate that the total volume of magma ejected during eruption of the Bishop tuff was of the order of 600 km^3.

Hildreth and Spera [1974] report on the basis of mineralogical and geochemical studies that the initial ash falls of the Bishop tuff erupted at temperatures of 745°C under a pressure of less than 2 kbar and that the ash flows erupted at 800°C under pressures of greater than 3 kbar. These data suggest that the roof of the chamber was at a depth of about 6 km at the time of initial outburst and that the last ash flows came from a depth of about 10 km. These data are in fair agreement with evidence to be discussed below, i.e., that the maximum amount of caldera collapse associated with the eruption of the Bishop tuff was about 3 km.

K-Ar ages on samples from three exposures of the Bishop tuff range from about 0.68 to 0.74 m.y. [*Dalrymple et al.*, 1965], but none of the individual measurements are significantly different from the weighted mean age of 0.708 ± 0.015 m.y. at the 95% level of confidence. Both the K-Ar ages and the paleomagnetic data, from welded parts of the Bishop tuff, are consistent with the interpretation that this ash flow sheet was emplaced within a time span of no more than a few centuries [*Dalrymple et al.*, 1965].

CALDERA SUBSIDENCE

As a result of eruption of the Bishop tuff the Long Valley magma chamber was partially emptied, and its roof consequently collapsed. Collapse probably took place along arcuate ring faults, although few of these are now exposed. One outer ring fault, with a maximum displacement of 250 m, can be traced for a distance of 12 km along the east wall of the caldera (Figure 3), but the gravity gradient on the eastern margin of the caldera [*Pakiser*, 1961; *Pakiser et al.*, 1964; *Kane et al.*, 1976] requires much greater displacement, and the main boundary fault must be buried in the caldera fill to the west. The main boundary fault probably lies well within the caldera moat, and the present diameter of the caldera undoubtedly has been enlarged by slumping of the initially unstable walls and by subsequent erosion.

Although *Gilbert* [1938, 1941] recognized Long Valley as the source of the Bishop tuff and suggested that most of the recent faulting in the depression was a result of extrusion of a large volume of magma from beneath it, the caldera origin of Long Valley has been questioned by some investigators, probably because the boundary faults are largely covered and actual displacement on them cannot be measured. The gravity studies of *Pakiser* [1961] and *Pakiser et al.* [1964] lent support to the caldera origin by more clearly defining its oval shape and establishing that it contained a great thickness of low-density fill. Pakiser (in the work by *Rinehart and Ross* [1964]) elaborated on the mechanism of eruption and collapse, but because he overestimated the volume of fill [*Kane et al.*, 1976], he concluded that volcanism alone could not account for the amount of subsidence, and consequently he considered Long Valley a volcano-tectonic depression. Recognition of a resurgent dome within the depression [*Smith and Bailey*, 1968] provided indirect evidence for caldera origin, but perhaps the most convincing evidence is that provided by the inclusions of Bishop tuff in the early rhyolites in the depression and by the timing of subsidence established by K-Ar dating. Bishop tuff inclusions in the early postcaldera rhyolite tuffs, which are at least 500 m thick, indicate that Bishop tuff has definitely subsided to a considerable depth within the depression (a minimum of 800 m below the general level of Bishop tuff on the north caldera rim). K-Ar dating (Figure 4) of the Bishop tuff (0.71 m.y.) and the earliest intracaldera rhyolites (0.73–0.68 m.y.) indicates that this subsidence occurred within a very short time following eruption of the Bishop tuff. Thus subsidence can clearly be associated with eruption of the Bishop tuff and is not the result of tectonic movements, which have been continuously active in the general area over a much longer time at much slower rates.

The minimum amount of subsidence of the cauldron block is about 1000 m, indicated by the topographic relief between the floor of Long Valley and the shoulders of Glass Mountain and remnants of the Tertiary erosion surface on the south rim of the caldera. The average thickness of low-density materials in the eastern half of the caldera beneath Long Valley, indicated by the gravity model of *Kane et al.* [1976, Figure 5] and by the seismic refraction study of *Hill* [1976], is about 3000 m. Of this thickness, 500–1000 m is probably downfaulted precaldera rhyolite of Glass Mountain. The caldera fill, including the Bishop tuff, in Long Valley is therefore about 2000–2500 m thick, so the maximum subsidence in the eastern part of the caldera is of the order of 3000 m.

The topographic relief on the walls in the west half of the caldera, about 300–600 m, is considerably less than in the east. Part of this difference may be accounted for by the infill of young basaltic lavas in the western moat, but they probably do not greatly exceed 200 m in thickness. The average thickness of low-density rocks in the western part of the caldera, indicated by *Kane et al.* [1976, Figure 5] and *Hill* [1976], is about 1700 m, of which about 200 m probably is precaldera volcanic rocks, judging from exposures in the west and north walls of the caldera. Thus the caldera fill, including Bishop tuff, in the west probably is about 1500 m, and the total subsidence is of the order of 2000 m. Subsidence in the west therefore is about 1000 m less than in the east.

This difference in subsidence in the east and west is especially evident in the gravity maps of *Kane et al.* [1976, Figures 2, 3], a conspicuous feature of which is a northwest-trending gradient transecting the middle of the caldera. This gradient coincides with the northward projection of the Hilton Creek fault, a major active Sierra Nevada frontal fault, and is thought to reflect either precaldera displacement of the basement (down to the east) on the intracaldera segment of the fault or, as suggested by *Hill* [1976], differential displacement on the fault during caldera collapse. It is also evident from the gravity and seismic refraction studies that the caldera fill thickens markedly to the north, suggesting that the floor tilted in that direction during subsidence.

The total volume of caldera subsidence can be estimated from the gravity model and the present topography. The volume of the present topographic depression, based on reconstruction of the precaldera topography, is about 200 km^3. The volume of the subsurface depression calculated from the gravity model [*Kane et al.*, 1976, Figure 3] is about 800 km^3 [*Muffler and Williams*, 1976]. Probably about one quarter of this volume is subsided precaldera volcanic rocks; hence the subsurface volume occupied by the Bishop tuff and younger rhyolite tuffs and lavas is about 600 km^3, and the total combined subsurface and topographic subsidence is of the order of 800 km^3. About 75% of this volume can be accounted for by the estimated 600 km^3 of magma ejected during eruption of the Bishop tuff, and possibly an additional 5–10% can be accounted for by minor subsidence accompanying eruption of post-caldera tuffs and lavas (40–80 km^3 of magma). Thus with presently available data, 80% or more of the estimated volume of subsidence can be attributed to eruption of the Bishop tuff and associated intracaldera volcanic rocks.

Early Rhyolites

K-Ar ages of 0.73–0.63 m.y. indicate that almost immediately after subsidence, eruptions resumed within the caldera. During this time crystal-poor rhyolite tuffs, domes, and flows accumulated on the floor to a thickness of at least 500 m. These rocks, informally designated the 'early rhyolites,' are exposed in tilted and uplifted fault blocks in the central part of the caldera.

The tuffs contain abundant inclusions of Bishop tuff and basalt and, less commonly, fragments of granitic and metamorphic rocks, indicating that all of these rock types occur within the cauldron block. Many of the rhyolite tuffs show varying degrees of reworking by water: low-amplitude cross-bedding, sorting, and grading. Although ripple marks are absent, the tuffs were very likely deposited, at least partly, in an early formed caldera lake.

The rhyolite domes and flows associated with the tuffs typically contain abundant jet black obsidian and have less than 3% phenocrysts of quartz, plagioclase, biotite, and hypersthene. The low crystal content of these lavas indicates that they erupted at near-liquidus temperatures. They also appear to have been unusually fluid for rhyolites, as some units less than 50 m thick flowed as far as 6 km. Three mineralogical facies have been mapped [*Bailey*, 1974]; in order of increasing phenocryst content and, in general, decreasing age, they are: (1) aphyric rhyolite, (2) pyroxene rhyolite, containing phenocrysts of quartz, plagioclase, hypersthene, and Fe-Ti oxide, and (3) biotite rhyolite, containing phenocrysts of quartz, plagioclase, hypersthene, biotite, and Fe-Ti oxide. Scarce phenocrysts of fayalite and augite also have been identified in some samples of biotite rhyolite. Available chemical data [*Rinehart and Ross*, 1964, Table 9; *Jack and Carmichael*, 1968, Table 1; R. A. Bailey, unpublished data, 1974] indicate that the early rhyolites typically contain about 75% silica and that the three facies are not appreciably different chemically, suggesting that the succession represents progressive crystallization of the same magma.

Twelve eruptive centers for the early rhyolites, many of them aligned on and offset by northwest-trending faults, are exposed in the central part of the caldera. Additional vents probably are buried in the caldera moat. *Kane et al.* [1976] interpret the arcuate chain of secondary lows in their gravity model as local accumulations of low-density materials. These lows quite possibly represent accumulations of coarse pumice around early rhyolite vents on outer caldera ring fractures. Evidence that early rhyolites are buried in the moat include (1) lithic aphyric rhyolite debris in the phreatic deposits of the Inyo craters; (2) aphyric rhyolite tuff uplifted on the side of a large rhyodacite dome in the southwest moat; and (3) pyroxene rhyolite beneath younger basalts in the northwest moat at 200 m depth in U.S. Geological Survey heat-flow hole (Figure 3, DC).

K-Ar measurements on 8 of the 12 early rhyolite domes and flows give ages of 0.73–0.63 m.y. (Table 1 and Figure 4). With only one exception the ages are consistent with the mapped stratigraphic succession: the exception is the apparent age of 0.73 m.y. on pyroxene rhyolite (location 6), which at the 95% confidence level is significantly older than the ages of either of the three dated aphyric rhyolites (locations 1, 10, and 13). None of the K-Ar ages of the early rhyolites are significantly older than the age of the Bishop tuff. The data indicate that (1) the early rhyolites were erupted during a span of no more than 100,000 yr and perhaps as little as 40,000 yr after eruption of the Bishop tuff and collapse of the caldera and (2) the pyroxene rhyolites may have been contemporaneous in part with the aphyric and biotite rhyolites.

Resurgent Doming

Contemporaneous with emplacement of the early rhyolites, the west central part of the caldera floor was uplifted and deformed into a subcircular structural dome. This resurgent dome [*Smith and Bailey*, 1962, 1968] is 10 km in diameter and consists of a mosaic of fault-bounded blocks that rise 500 m above the surrounding moat. The dome is transected by a 5-km-wide complexly faulted keystone graben that trends northwest. The early rhyolites exposed in the dome are tilted radially outward as much as 30°, and detailed mapping of flow foliations and lineations [*Chelikowsky*, 1940; *Bailey*, 1974] shows that most of the extrusive units flowed radially away from the geometric center of the dome. Evidence that the dome is the result of positive central uplift rather than differential collapse of the moat is as follows: (1) lake terraces tilted outward on the dome at elevations as much as 35 m higher than the highest terrace on the caldera walls; (2) scattered beach pebbles as much as 80 m higher on the dome than on the caldera walls; and (3) 1- to 2-m-diameter blocks of granitic and metamorphic rocks, interpreted as ice-rafted glacial erratics from the Sierra Nevada [*Rinehart and Ross*, 1964, p. 68], 200 m higher on the dome than the highest terrace on the caldera walls and 60 m higher than the lowest part of the caldera rim during early postcaldera time. These features also indicate that the resurgent dome was an island in a caldera lake during much of its history (see Figure 5).

The orientation of the keystone graben in the resurgent dome is undoubtedly controlled by the dominant northwest trend of regional structures along the east front of the Sierra Nevada. The eccentric location of the resurgent dome is thought to be controlled by lines of structural weakness within the Mount Morrison roof pendant, which probably continues in the basement northwestward through the cauldron block to exposures of metamorphic rock on the north wall of the caldera near Big Springs. Several major precaldera faults within and bounding the roof pendant, the Hilton Creek, McGee Mountain, and Laurel-Convict faults [*Rinehart and Ross*, 1964, Plate 1] (Figure 3), undoubtedly contributed to the weakness of this zone.

Decrease in the amount of radial tilting of progressively younger flow units on the dome suggests that uplift was waning toward the close of eruption of the early rhyolites. However, no units between 0.63 and 0.51 m.y. old have been dated, so the time of termination of doming is not precisely known. The top of a 0.51-m.y.-old hornblende-biotite rhyolite dome (location 12) on the north flank of the resurgent dome slopes gently to the north, but whether this is due to posteruption tilting or to slumping during extrusion onto a preexisting slope is uncertain. A 2280-m (7500 ft) lake terrace that laps against this dome does not appear to be tilted, nor do the many other lower terraces and strandlines down to 2140 m (7000 ft) on the north slope of the resurgent dome. Thus doming, which began shortly after collapse of the cauldron, continued until about

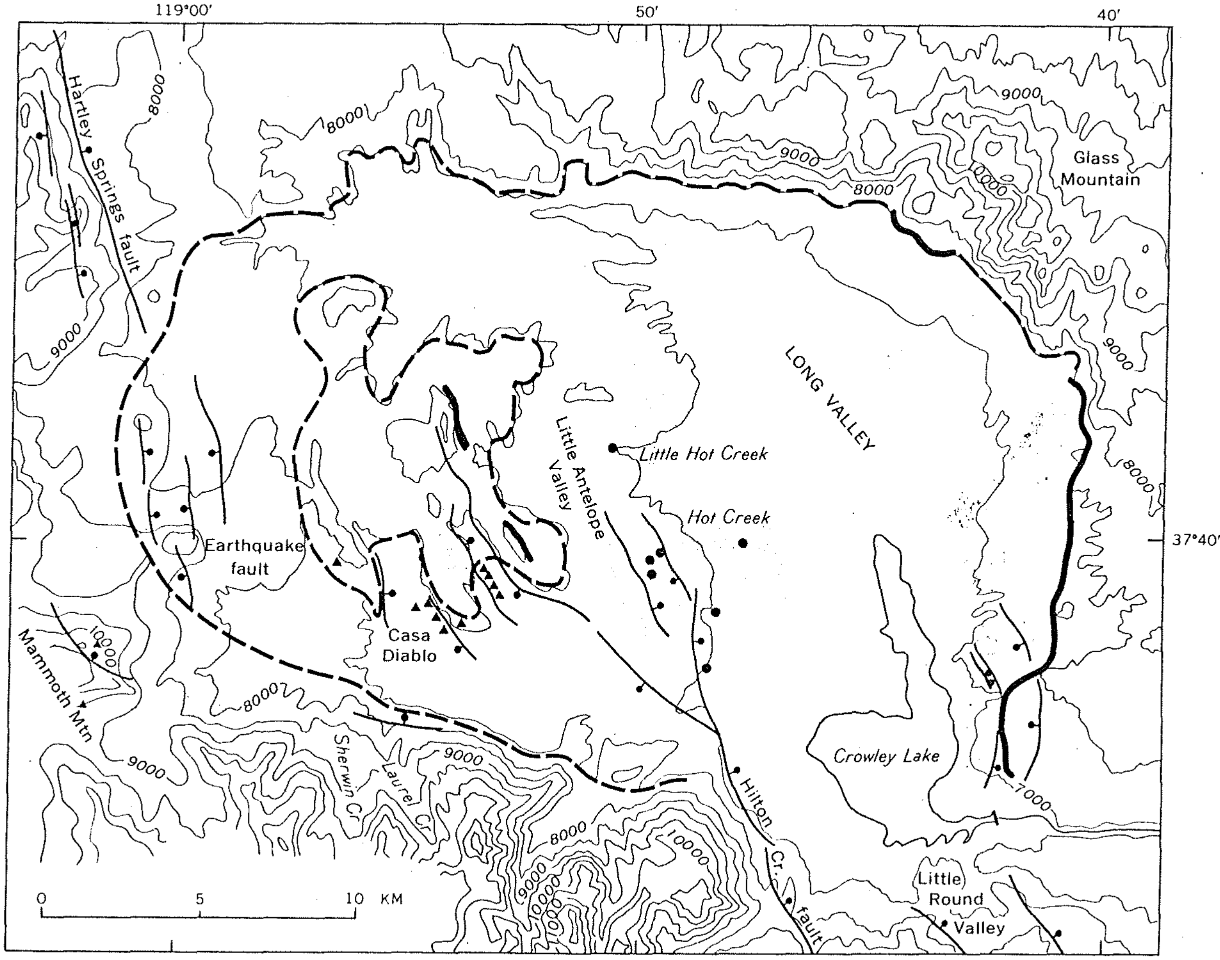

Fig. 5. Maximum extent of Pleistocene Long Valley Lake and distribution of hydrothermal activity. The heavy solid line represents remnants of highest (2320 m (7600 ft)) lake terrace; heavy dashed line, inferred position of highest shoreline and maximum extent of lake; triangles, active fumaroles; solid circles, active hot springs; dotted area, distribution of fossil gas vents and hydrothermal alteration; and solid thin lines, recently active faults. Contour interval is ~150 m (500 ft).

0.63 m.y. ago but probably did not persist much beyond 0.51 m.y. ago.

MOAT RHYOLITES

After resurgence, coarsely porphyritic hornblende-biotite rhyolite erupted from three groups of vents in the caldera moat. These rhyolites, informally designated the 'moat rhyolites,' are highly pumiceous and contain as much as 20% phenocrysts of hornblende, biotite, quartz, sanidine, and plagioclase. A single chemical analysis from a dome in the west moat indicates that they have silica contents of about 72% [*Rinehart and Ross*, 1964, Table 1]. They typically form steep-sided domes or thick flows of limited extent. Their crystal content and geomorphic form indicate that they were more viscous and probably erupted at lower temperatures than the early rhyolites.

The oldest hornblende-biotite rhyolites erupted on the north flank of the resurgent dome where two of four centers have been dated at 0.509 ± 0.011 m.y. (location 12) and 0.468 ± 0.010 m.y. (location 11). A second group of five erupted in the southeast moat, three of which have been dated at 0.349 ± 0.006 m.y. (location 25), 0.324 ± 0.010 m.y. (location 5), and 0.28 ± 0.03 m.y. (S17 of *Doell et al.* [1966]). A third group of four, with K-Ar ages of 0.113 ± 0.004 m.y. (location 17), 0.106 ± 0.003 m.y. (location 7), 0.103 ± 0.002 m.y. (location 9), and 0.094 ± 0.006 m.y. (location 8), occurs in the west moat. Thus the three groups erupted about 0.5, 0.3, and 0.1 m.y. ago in clockwise succession around the resurgent dome. These rocks are temporally, spatially, and petrographically analogous to the ring domes of the Valles caldera, New Mexico [*Smith and Bailey*, 1968; *Doell et al.*, 1968], and their distribution is probably controlled by ring fractures that bound the resurgent dome. The presence of hydrous minerals and the greater vesicularity of the moat rhyolites suggest that their extrusion and reopening of the ring fractures may have been caused by the concentration of volatiles accompanying crystallization of the magma and consequent increase in volatile pressure in the chamber. The apparent 0.2-m.y. periodicity of the groups may be a measure of the time required to build up sufficient pressure to reopen the ring fractures.

The restriction of the centers to three distinct areas in the ring fracture zone may be due to the fact that in these areas the ring fractures intersect major northwest-trending precaldera faults within the cauldron block. This suggestion is further supported by the northwest alignment of some of the domes within the groups. In the northern group, four vents are spaced at 1.5-km intervals on a northwest trend that may be either an arc concentric to the margin of the resurgent dome or a northwest extension of the Hilton Creek fault. The five vents of the southeast group appear to be randomly distributed, but they also are in the general area of intersection of the Hilton Creek fault with the ring fracture zone. The three main domes of the western group are aligned north-northwest parallel to minor intracaldera faults that are in line with the Hartley Springs fault northwest of the caldera. The fourth dome in this group, Deer Mountain, although isolated from the other three, is aligned with the younger Inyo domes, which also trend north-northwest parallel to the Hartley Springs fault.

RIM RHYODACITES

Hornblende-biotite rhyodacites, less silicic and richer in crystals than the hornblende-biotite rhyolites of the caldera moat, occur at three localities on the caldera rim or in the outer part of the caldera moat: (1) Mammoth Mountain on the southwest, (2) Deadman Creek on the northwest, and (3) the foot of Glass Mountain on the northeast. A fourth unvented rhyodacite (?) intrusion probably occurs at the foot of Bald Mountain on the north, where cemented conglomeratic sediments capped with travertine have been punched upward into a steep-sided structural dome about 1 km in diameter. It is difficult to account for this structure other than by intrusion of a small igneous plug. Because of their peripheral location and semiarcuate distribution, these rhyodacites are informally designated the 'rim rhyodacites.'

Mammoth Mountain, the largest and most imposing of these rhyodacite centers, is a complex cumulo-volcano, consisting of many superimposed domes and short thick flows. At least 10 major eruptive vents can be identified on the mountain, most of which occur within an arcuate zone parallel to the caldera wall. The northeast face of the mountain has been oversteepened by glaciation and also in part by faulting. Displacement of lavas across a conspicuous cleft high on the northeast side of the mountain suggests that the northeast half of the mountain has subsided (see section on postcaldera tectonic activity).

The lavas of Mammoth Mountain have silica contents ranging from 74 to 66% [*Huber and Rinehart*, 1967, pp. D14–D15, Figure 5]. Recent mapping by R. P. Koeppen (personal communication, 1973) shows an upward succession from biotite rhyolite through biotite-augite rhyodacite to hypersthene-hornblende rhyodacite, indicating a trend toward more mafic compositions with time and suggesting that the lavas may have erupted from a high-level differentiated cupola.

The rhyodacites of Deadman Creek were mapped by *Rinehart and Ross* [1964] and *Huber and Rinehart* [1967] as 'olivine-bearing quartz latite.' These rocks comprise three small lava domes and a flow. The three domes are hornblende-biotite rhyodacites mineralogically similar to those of Mammoth Mountain and have silica contents of 63–67%. The associated flow, the only unit that contains olivine, has a lower silica content, 59–61% (N. K. Huber and C. D. Rinehart, personal communication, 1974), and is mineralogically heterogeneous, with olivine, augite, hypersthene, biotite, hornblende, plagioclase, sanidine, and quartz crystals, all in varying stages of reaction with the enclosing brown glass. Such relations suggest that the rock is the product of intermixing of rhyodacitic and basaltic liquids, a distinct likelihood since the K-Ar data indicate that basalts and rhyodacites were erupted contemporaneously in the western moat.

The small rhyodacite dome at the base of Glass Mountain has been described by *Gilbert* [1941, p. 799] as 'andesite,' but its mineralogy indicates that it is more silicic than typical andesites of the region. The rock contains abundant small crystals of hornblende and plagioclase in a light gray glassy matrix; its composition probably does not differ much from the rhyodacites of Deadman Creek and Mammoth Mountain.

It is probably not accidental that the two largest accumulations of rhyodacite, Mammoth Mountain and the Deadman Creek domes, occur where the caldera rim is intersected by a north-trending fracture system that also localized the more widely distributed, contemporaneous basalts described in the following section. The intersection of this fracture system with the outer caldera rim fractures undoubtedly was a zone of weakness that preferentially channeled magma to the surface. However, the fact that one and possibly two other rhyodacite centers occur along the north wall of the caldera, well to the east of this fracture zone, suggests that the rhyodacites are genetically related to the Long Valley magma chamber and not to the more deeply derived basalts.

Four rhyodacites have been dated in this study, two of which are among the youngest in the Mammoth Mountain complex. One from the summit dome (location 29) has an apparent sanidine age of 0.050 ± 0.010 m.y., and one from a flow midway down the northern flank (location 30) gives a biotite age of 0.118 ± 0.048 m.y. Two additional rhyodacites near Mammoth Mountain, a dome (location 27) and a flow (location 26), give K-Ar ages on biotites of 0.138 ± 0.079 m.y. and 0.145 ± 0.029 m.y., respectively. Previously published K-Ar ages from Mammoth Mountain include one of 0.148 ± 0.049 m.y. on biotite [*Curry*, 1971] and two on the same dome, 0.18 ± 0.09 m.y. on biotite [*Huber and Rinehart*, 1967] and 0.37 ± 0.04 on plagioclase [*Dalrymple*, 1964*a*]. Petrographic studies indicate that the plagioclase phenocrysts in the Mammoth Mountain rocks have had complex histories and probably have xenocrystic cores. Preliminary results of K-Ar dating of coexisting biotite and plagioclase from other Mammoth Mountain rocks show that K-Ar ages of plagioclase are more variable and consistently older than those on coexisting biotite, suggesting that biotite ages more closely reflect eruptive ages. If so, the rocks on Mammoth Mountain probably are no older than 0.18 ± 0.09 m.y.

These age data indicate that Mammoth Mountain was active for a minimum of about 100,000 yr and that rhyodactic volcanism was partly contemporaneous with the western group of moat rhyolites, as well as with the basalts described below.

LATE BASALTIC VOLCANISM

The west moat of Long Valley caldera contains many basaltic flows and cinder cones that are part of a more extensive chain of mafic volcanic rocks extending from southwest of Mammoth Mountain 45 km northward into Mono basin. This chain includes the trachybasaltic rocks of the Devils Postpile [*Huber and Rinehart*, 1967], the trachyandesite cinder cones and flows of the June Lake area [*Putnam*, 1949], and the sublacustrine cinder cone of Black Point on the north shore of Mono Lake [*Christensen and Gilbert*, 1964; *Lajoie*, 1968]. These rocks appear to have erupted from a north-trending fracture system consisting of north-northwest-trending en echelon segments that parallel the east front of the Sierra Nevada. Chemically and mineralogically, the rocks are similar to Cenozoic mafic rocks that occur throughout the Basin and Range province [*Leeman and Rogers*, 1969], and presumably they have a similar origin.

In general, the ages of the rocks decrease northward in the chain. The oldest rocks are from the Devils Postpile area, where K-Ar measurements on two different plagioclase separates from the same sample give ages of 0.63 ± 0.35 m.y. [*Huber and Rinehart*, 1967] and 0.94 ± 0.16 m.y. [*Dalrymple*, 1964*b*]. K-Ar ages on nine intracaldera basalts and trachyandesites range from about 0.2 to 0.06 m.y. (Table 1, Figure 4). North of the caldera, the trachyandesite near June Lake overlies Tahoe till and is overridden by Tioga till [*Putnam*, 1949]; hence it is probably between 75,000 and 20,000 yr old [*Curry*, 1971]. The Black Point cinder cone on the north shore of Mono Lake is dated at 13,300 ± 500 yr by ^{14}C on ostracods from interbedded sediments [*Lajoie*, 1968].

The K-Ar ages of the basaltic rocks within Long Valley caldera indicate that basaltic volcanism was contemporaneous with the younger hornblende-biotite rhyolites of the western moat as well as with the rim rhyodacites. Since it is unlikely that liquid basalt could have penetrated any part of the rhyolitic magma chamber that had not already solidified, the distribution and age of the intracaldera basaltic centers are important indicators of the extent of crystallization of the Long Valley chamber. The innermost basaltic center in the western moat is 4 km from the caldera walls and is dated at 0.222 ± 0.080 m.y. (location 18). Thus at that time the chamber presumably had solidified inward at least 4 km from its margins and roof. The dimensions and geometry (thickness-diameter ratio) of the resurgent dome [*Smith and Bailey*, 1968, p. 646] suggest that at the close of resurgence about 0.6 m.y. ago the roof of the chamber probably was not deeper than 5 km and possibly was as shallow as 2 or 3 km. Thus about 0.2 m.y. ago the chamber had congealed to a depth of 6–9 km from the surface.

Of special interest to the glacial geology of the area are K-Ar ages of three basaltic flows exposed in the south moat. A till, named the Casa Diablo till by *Curry* [1971], is found between the middle and lower of these flows. On the basis of single K-Ar ages of 0.192 ± 0.035 m.y. on the upper flow, 0.280 ± 0.067 m.y. on the middle flow, and 0.441 ± 0.040 m.y. on the lower flow, Curry assigned the Casa Diablo till an age of about 0.4 m.y. and a stratigraphic position between the Sherwin till [*Sharp*, 1968] and the Mono basin till of possible Illinoian age [*Sharp and Birman*, 1963]. We have made duplicate measurements on the upper and lower of these three flows and obtained considerably different results. On the basis of our data the age of Curry's Casa Diablo till is between 0.062 ± 0.013 m.y. (location 23) and 0.126 ± 0.025 m.y. (location 22) and therefore may be equivalent in age to Mono basin till.

HOLOCENE RHYOLITIC VOLCANISM

The youngest volcanic features in Long Valley caldera are the Inyo craters and domes, [*Mayo et al.*, 1936], which are aligned on an apparent north-trending fracture extending from the west moat to the Mono craters along the east front of the Sierra Nevada. The Inyo domes are five rhyolitic to rhyodacitic lava domes, the three largest of which are the youngest (less than 720 ± 90 yr old on the basis of ^{14}C dating [*Wood*, 1975]). The Inyo craters are three phreatic explosion pits on the south flank of Deer Mountain (the moat rhyolite just south of the southernmost Inyo dome) and have been dated by ^{14}C at 650 ± 200 yr [*Rinehart and Huber*, 1965]. No primary ash or lava was expelled during formation of the craters, and very probably they were caused by rhyodacitic magma rising to shallow depth and flashing groundwater to steam. Thus it is possible that residual rhyodacitic magma was present in the Long Valley chamber as recently as 450 yr ago (see also *Steeples and Iyer* [1976]).

The Inyo domes are of particular interest because they are chemically and physically heterogeneous [*Lajoie*, 1968, p. 140; *Jack and Carmichael*, 1968, p. 22]. The three youngest domes are fluidal mixtures of two distinctly different rock types: (1) light, coarsely porphyritic hornblende-biotite rhyodacite that tends to be pumiceous, and (2) dark, sparsely porphyritic rhyolitic obsidian. The rhyodacite mineralogically and texturally resembles the rhyodacites of Long Valley caldera, whereas the rhyolitic obsidian resembles that of the Mono craters. Moreover, from north to south approaching Long Valley caldera, the proportion of pumiceous rhyodacite in successive domes increases noticeably at the expense of the obsidian, a relation that suggests that the Inyo domes represent the mixing along a north-south fissure of magmas from the Long Valley chamber and a chamber beneath the ring fracture zone of the Mono craters (Figure 1) [*Kistler*, 1966*b*, p. E48]. The age (about 12,000–1300 yr) and frequency of eruption of the Mono craters [*Dalrymple*, 1967; *Friedman*, 1968] suggest that the subjacent chamber may be actively rising and capable of feeding further eruptions.

PLEISTOCENE LONG VALLEY LAKE

After caldera subsidence the Long Valley depression was filled with water to form Pleistocene Long Valley Lake [*Mayo*, 1934]. Although normal runoff within the drainage basin was probably sufficient to fill the depression in a relatively short time, it is likely that glaciers were present in the Sierra Nevada at that time and that runoff was greatly accelerated by melting caused by the blanket of hot ash laid down during eruption of the Bishop tuff. This caldera lake rose to a level of at least 2320 m (7600 ft), as indicated by remnants of terraces on the northeast and east walls of the caldera (Figure 5). Terraces and strandlines are exceptionally well developed along the east wall, where they can be traced continuously for 14 km and where they have been downwarped southward and locally faulted. The terraces are veneered with coarse sand and gravel, consisting predominantly of well-rounded cobbles and pebbles of obsidian and lithoidal rhyolite, locally cemented with carbonate. This detritus was derived from the reworking of the tuffs and epiclastic sediments of Glass Mountain, which are exposed in the east rim and wall of the caldera. The gravels also contain scattered, large, angular blocks of coarsely porphyritic Cathedral Peak–type granite and metavolcanic rocks. The only source for these blocks is in the Sierra Nevada southwest of the caldera [*Huber and Rinehart*, 1965], so they must have been ice-rafted across Long Valley Lake. As noted in a preceding section, erratics of apparently similar origin are found on the west and south flanks of the resurgent dome within the caldera. These are the windward flanks against which icebergs from the Sierran glaciers would most likely have lodged.

Calcareous cement is common in the gravels of the lower terraces, and on the lowest terraces, dense, finely crystalline, calcareous tufa deposits are extensively developed. The increase in the amount of cementation and in the thickness of tufa on successively lower terraces suggests either more enduring lower lake stands, increased algal activity, or progressive increase in alkalinity and salinity of the lake water with time, the latter possibly due to late Pleistocene desiccation or to increased introduction of alkalies and salts from hot springs during the later part of the caldera history. Absolute dating of the terraces using the hydration rind method [*Friedman and Smith*, 1960] on obsidian pebbles is in progress and perhaps will provide further information on the history of the lake and its chemical evolution.

Draining of the caldera lake was attributed by *Mayo* [1934] and *Putnam* [1960] to headward cutting by the Owens River, but it is more likely that drainage was initiated by overflow of the lake, as was believed by F. E. Matthes [see *Putnam*, 1960, p. 248]. The lake probably rose rapidly, forming no terraces during its rise to the lowest point on the caldera rim, which at that time was at about 2380-m (7800 ft) elevation and near the present lake outlet. It then began overflowing across the surface of the Bishop tuff, cutting rapidly downward through the upper 60 m or so of nonwelded to partly welded tuff, until it reached the densely welded zone at 2320 m (7600 ft), where the lake level became temporarily stabilized. (An ancient stream valley preserved in the surface of the Volcanic Tableland 20 km to the southeast [*Bateman*, 1965, p. 167] was probably cut by this early outflow stream.) The 2320-m (7600 ft) level coincides with the highest terrace recognized on the northeast caldera wall. (A figure of 2410 m (7900 ft) has been repeatedly cited in the literature for the highest lake terrace, but the surface rising to this elevation is an alluvial fan, not a terrace; the highest well-rounded beach pebbles indicating a lake strand are at 2320 m (7600 ft).) Since initial stabilization of the lake, overflow has been controlled by downwarping and intermittent movement on faults that bound the east front of the Sierra Nevada and intersect the caldera rim. (See section on post-caldera tectonic activity.)

That the lake reached a high level early in its history is indicated by the fact that many of the early rhyolites exposed in the resurgent dome are pervasively hydrated, suggesting their eruption into the caldera lake. Critical in this respect are two flows on the north flank of the resurgent dome, one being a pervasively perlitized biotite rhyolite flow and the other an overlying obsidian-bearing pyroxene rhyolite flow (location 14) dated at 0.634 ± 0.013 m.y. The pyroxene rhyolite, the youngest dated flow on the resurgent dome, is not greatly tilted or uplifted and is exposed at elevations from 2320 m (7600 ft) to 2415 m (7920 ft). The perlitized biotite rhyolite apparently flowed into the lake, whereas the overlying pyroxene rhyolite did not. Thus the lake probably reached its highest level, presumably 2380 m (7800 ft), near the time of eruption of the biotite rhyolite and then receded to 2320 m (7600 ft) before eruption of the pyroxene rhyolite flow 0.63 m.y. ago.

The approximate position of successively lower and younger lake levels may be inferred from other dated volcanic units within the caldera (Figure 6). On the north flank of the resurgent dome, lake terrace deposits at an elevation of 2290 m (7500 ft) lap against the base of a hornblende-biotite rhyolite dome (location 12) dated at 0.509 ± 0.011 m.y. but do not occur on an adjacent agglutinate cone and lava flow (location 11) dated at 0.468 ± 0.010 m.y.; the highest terrace deposits on the latter occur at 2230 m (7300 ft). Thus the lake level apparently was near 2290 m (7500 ft) between 0.51 and 0.47 m.y. ago and receded to 2230 m (7300 ft) after 0.47 m.y. ago.

Lake sediments above and below the Hot Creek rhyolite flow (S17 of *Doell et al.* [1966]) in the southeast moat indicate that the lake surface was at about 2200 m (7200 ft) about 0.28 m.y. ago. Lack of evidence that the basalt in the north moat (location 20) flowed into water indicates that the lake was below 2135 m (7000 ft) 0.104 m.y. ago. Complete draining of the lake occurred sometime within the last 0.1 m.y. (Lake Crowley is not a remnant of Pleistocene Long Valley Lake but is impounded behind Crowley Dam, which was built in 1941.)

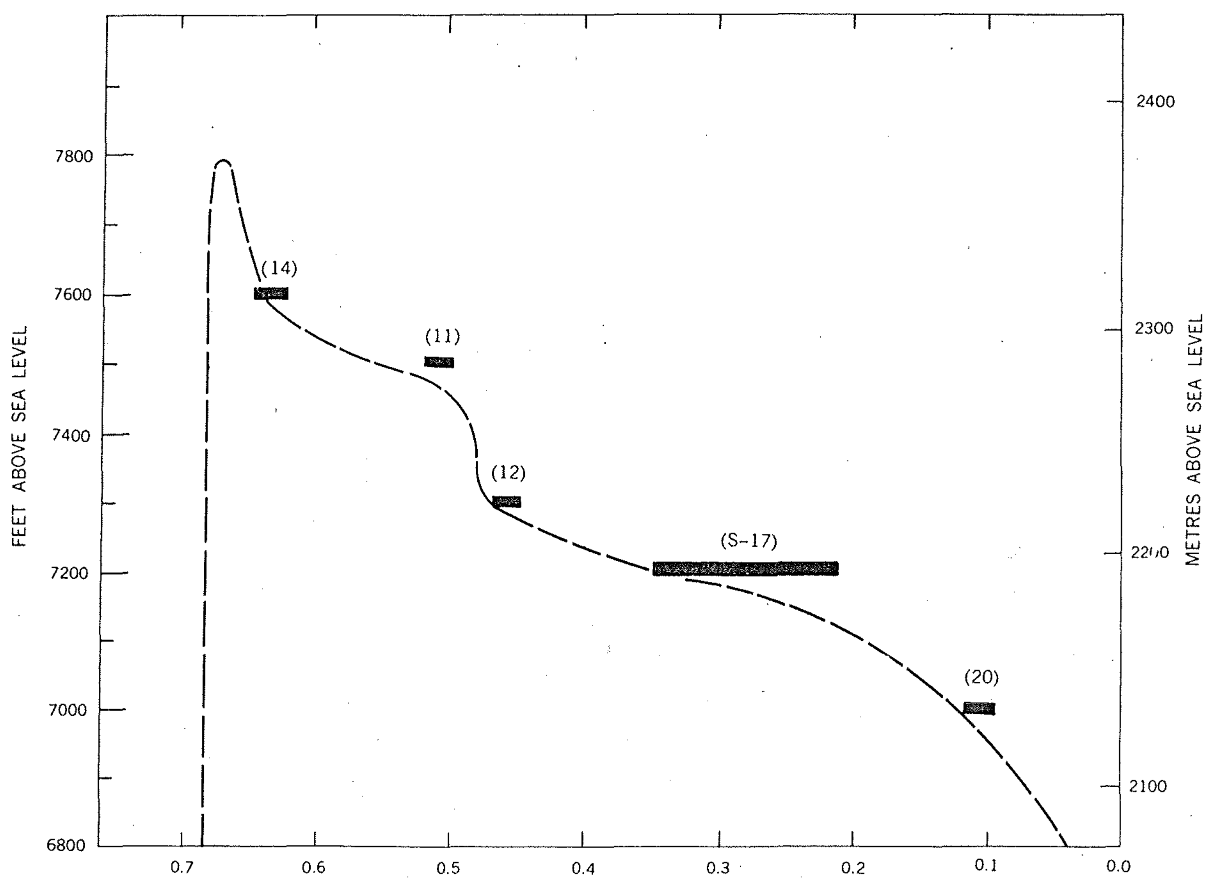

Fig. 6. Elevations and ages of Pleistocene Long Valley Lake levels. Dashed line shows general rise and fall of lake level with time, based on age of associated volcanic unit (solid bar). Numbers in parentheses are locality numbers of dated samples (Table 1 and Figure 3). Length of bar is analytical error of age determination.

LACUSTRINE SEDIMENTS

The sediments within Long Valley have been exposed to a depth of only 50 m by the dissection that followed draining of the caldera lake, and the deepest penetration of them by drilling is 305 m in U.S. Geological Survey drill hole LVCH-1 (Figure 3). Consequently, little is known of the character of the deeper sedimentary fill, although a large portion of it is undoubtedly lacustrine.

The upper 50 m of sediment exposed on the east flank of the resurgent dome are predominantly pebble conglomerate and coarse tuffaceous sandstone. They contain abundant clasts of early rhyolite indicating that they were derived mainly from erosion of the resurgent dome. The sediments commonly exhibit deltaic structure with well-developed topset and foreset beds, the latter having dips as much as 30° and amplitudes of as much as 10 m [*Rinehart and Ross,* 1964, pp. 76–77, Figure 38]. The topset beds commonly grade upward into marsh deposits containing or locally consisting almost entirely of silicified reedlike plant stalks and rootlets. Eastward the marsh and deltaic deposits grade or interfinger with fine-grained buff to white diatomaceous sediments exposed in the lower parts of Long Valley. Ostracods are abundant in both marsh and diatomaceous deposits.

In drill hole LVCH-1 the sediments below 50 m tend to be somewhat coarser and more pumiceous, but the general lithology does not change conspicuously downward, and no particularly distinctive units were penetrated. The Bishop tuff was not intersected, and it undoubtedly lies at much greater depth. Below 150 m the sediments in the drill hole are zeolitized. The principal zeolite is clinoptilolite, which occurs as a replacement product of glass shards and pumice; below 250 m, heulandite is also present as fine crystals in cavities. The sediments penetrated by the drill hole dip gently, usually not more than 10°, but several zones, each about 5 m thick, show intensely contorted and thrusted bedding, suggesting that penecontemporaneous wet sediment slumping, possibly triggered by earthquakes, was an important sedimentation process.

HYDROTHERMAL ACTIVITY

On the east and southeast flanks of the resurgent dome the tuffaceous lacustrine sediments are locally intensely argillized as a result of acidic hydrothermal alteration by hot spring and fumarolic activity. This argillization is most intensely developed in the vicinity of Little Antelope Valley and upper Little Hot Creek, although smaller areas also occur near Hot Creek, Casa Diablo, and northeast of Mammoth Lakes on the southwest edge of the resurgent dome. These argillized areas have not been studied in detail as yet, but they apparently consist mainly of kaolinite with traces of montmorillonite and alunite [*Cleveland*, 1962]. The kaolin deposits near Little Antelope Valley are of commercial grade and have been actively mined since the early 1950's. In the deeper parts of the Little Antelope Valley clay quarry, tuffaceous and conglomeratic sediments, initially consisting of clasts of lithoidal rhyolite, obsidian, and pumice, are completely argillized, yet bedding and clastic textures are almost perfectly preserved. In the upper part of the quarry the sediments are also opalized, and layers of opal become progressively thicker and more abundant upward. The origin of this type of zonation has been explained by *Schoen et al.* [1974] as the result of incongruent dissolution of primary minerals above the groundwater table by downward percolating sulfuric acid waters generated by near-surface oxidation of H_2S-bearing fumarolic gas. This process apparently ceased some time ago in the Little Antelope Valley area, as there are no active fumaroles nearby at present, although temperatures are rather high (110°C) at depths of 165–200 m in U.S. Geological Survey drill hole LVCH-6, 1 km south of the clay quarry [*Lachenbruch et al.*, 1976*b*].

Surrounding and locally overlying these areas of acid alteration, the lacustrine sediments are thoroughly cemented with opal but are otherwise unaltered. They form a hard, resistant cap rock as much as 15 m thick. The temporal and genetic relation between these silica-cemented sediments and those that are argillized and partly replaced by opal is unclear, but the silica-cemented sediments contain myriads of vertical pipelike or honeycomblike structures (illustrated by *Cleveland* [1962, Figure 8]) that have been identified as fossil gas vents (L. J. P. Muffler, personal communication, 1972). These interesting structures suggest that the sediments were deposited over an active fumarolic area, possibly during a temporary rise of the caldera lake. Also, locally interbedded with these silica-cemented sediments, mainly along faults, are now-inactive siliceous sinter deposits.

The wide distribution of these fossil gas vents, ancient sinter deposits, and areas of acid alteration (Figure 5) indicates that surficial hydrothermal activity within the caldera was more extensive as well as more intensive in the past than at present, and we suspect that parts of Long Valley were formerly as active as some of the Yellowstone geyser basins are today. The apparent decline and areal restriction of surficial hydrothermal activity are probably due to the general reduction in permeability of the intracaldera rocks and sediments by silicification, argillization, and zeolitization. These 'self-sealing' processes [*White et al.,* 1971] have progressed to a depth of at least 300 m, as indicated by the impermeability of sediments cored in drill hole LVCH-1. Although in detail the interrelations between these three types of alteration appear to be complex in the field, their general distribution and relative depths suggest a zonation downward from silicification at the surface through argillization to zeolitization at depth. This zonation is probably a function mainly of increasing temperature with depth, and the complexities observed probably are due to fluctuations in groundwater levels related to rising and falling of the caldera lake and to recurrent fracturing of the cap rock by tectonic activity.

Rinehart and Ross [1964, p. 80] have pointed out that most of the active hot springs and fumaroles are located on or near north- to northwest-trending faults. The only apparent exception is the springs along Hot Creek, which are aligned northeast along the bottom of the gorge. These springs, however, are confined within a shallow, 2-km-wide, northwest-trending graben, and their northeast alignment is the result of their flowing from the permeable, brecciated base of the Hot Creek rhyolite flow, which is confined to the gorge bottom. Significantly, the hottest springs, some of which are boiling, occur only near the two main faults bounding the graben; the cooler springs in the center of the graben are probably the result of lateral migration of fluid through the basal breccia of the flow or along minor graben fractures, where mixing with cold surface waters occurs.

Most of the hot springs and fumaroles in Long Valley are on active extensions of the Hilton Creek fault, which suggests that their location is related to disruption of the 'self-sealed' moat sediments by this relatively active Sierra Nevada frontal fault. An apparent temporal as well as spatial relation between faulting and hot spring activity was dramatically demonstrated recently when new boiling springs and ephemeral geysers erupted along Hot Creek within hours of two earthquakes on August 25, and October 17, 1973. Although the epicenters were 20–40 km distant and not on the Hilton Creek fault, it seems likely that tremors disturbed the delicate plumbing of springs on the Hilton Creek system. The activity of the new springs and geysers has diminished markedly since their outbreak, but many of the older springs along Hot Creek and on Little Hot Creek, 3.5 km to the north, have shown marked increases in flow, and some an increase in temperature also, suggesting that their channels have been selectively enlarged since the earthquakes. With the data of *Haas* [1971] the salinities (~0.1%) and the geochemically indicated reservoir temperatures (~200°C) of the new hot spring waters [*Mariner and Willey*, 1976] suggest that they originated from a depth of at least 150 m. The presence of detrital zeolite particles in the new spring waters suggests a similar minimum depth of origin, as zeolites occur only below 150 m in drill hole LVCH-1, 1.5 km north of the new springs.

Although more sparsely distributed than in the east and south, hydrothermal activity also occurs locally in the western part of the caldera. Active fumaroles and abundant acid alteration occur on Mammoth Mountain [*Huber and Rinehart*, 1967, p. D19], a zone of hydrothermal alteration parallels the southwest caldera wall near the base of Mammoth Rock [*Rinehart and Ross*, 1964, p. 81], and pyritized rhyolite occurs at a depth of 210 m in U.S. Geological Survey heat-flow drill hole DC in the northwest moat (Figure 3). The apparent paucity of hydrothermal activity at the surface in the western moat does not necessarily indicate a lack of activity at depth because the thick sequence of young basalts in the western moat and the abundant subsurface flow of cold water from the Sierra Nevada may mask it.

Although individual hot springs and fumaroles are associated locally with north- to northwest-trending faults and fractures, the general distribution of hydrothermal activity within the caldera is in an arcuate zone peripheral to the resurgent dome, suggesting that the dominant controlling structures at depth are the caldera ring fractures. It is noteworthy that fumaroles in Long Valley caldera are restricted to fractures within the keystone graben of the resurgent dome, whereas hot springs are at lower elevations marginal to the dome where the groundwater table is near or at the surface.

Although fumaroles and hot springs probably have been active locally to a minor degree throughout the history of the caldera, the extensive development of hydrothermal activity in lacustrine sediments that are about 0.3 m.y. old, judging from the 0.28-m.y. age of the interbedded Hot Creek rhyolite flow, suggests that the geothermal system may have reached maximum development at about that time. This notion seems to be supported by the paucity of evidence for hydrothermal activity directly associated with the 0.73- to 0.63-m.y. early rhyolites and the 0.5-, 0.3-, and 0.1-m.y. moat rhyolites. This implies that the geothermal system is not related to the individual postcaldera eruptive groups but to the main magma chamber, which is a deeper and larger heat source. It also suggests that development of the geothermal circulatory system may have required considerable time and been completed only during the latter part of the caldera history.

Postcaldera Tectonic Activity

Matthes [1933, 1939], *Christensen* [1966], *Bateman and Wahrhaftig* [1966], and others have concluded that the rise of the Sierra Nevada crest was essentially completed before the advent of Pleistocene glaciation and that development of the eastern escarpment is the result of downfaulting of the region to the east during the past 3 m.y. Long Valley caldera lies across the faulted front of the Sierra and is intersected on the northwest and southeast by major frontal faults that have been active in both precaldera and postcaldera time. Because it is almost certain that the Long Valley magma chamber was substantially molten during this time, it is of interest to consider how the chamber responded to and how it may have influenced this tectonic activity locally.

The northwest caldera wall is intersected by the Hartley Springs fault (Figure 5), which has displaced precaldera andesites of the Tertiary San Joaquin Mountain complex by 450 m and the Bishop tuff by about 300 m. The topographic relief on the escarpment is about 600 m. This fault scarp terminates at the northwest caldera rim; southward within the western caldera moat several minor en echelon faults project on strike with it and form an ill-defined, incipient graben that terminates in the 'earthquake fault' [*Benioff and Gutenburg*, 1939] near the northeast base of Mammoth Mountain. These en echelon faults displace 0.2-m.y.-old trachyandesites by about 15 m, 0.1-m.y.-old moat rhyolite by about 10 m, and 650-yr-old Inyo crater phreatic deposits by about 5 m. Topographic evidence also indicates that the floor of western moat east of these faults is about 60 m lower than to the west. However, there is no suggestion of displacement in the west moat of 600 m as on the Hartley Springs fault outside the caldera. Thus the intracaldera segment or trace of the Hartley Springs fault appears not to have been active until fairly recent time.

The southeast caldera rim is intersected by the Hilton Creek fault, which forms an 1100-m escarpment at the mouth of McGee Creek. What part of this escarpment can be attributed to postcaldera movement is not precisely determinable, but if the fault has been continuously or intermittently active, it probably amounts to several hundred meters, as displacement on Tioga lateral moraines and outwash at the mouth of McGee Creek is as much as 15 m [*Putnam*, 1962, p. 200]. Like the Hartley Springs fault, the Hilton Creek fault terminates as a major escarpment at the caldera wall; within the caldera it splinters into several minor diverging faults that die out northward. The largest and most continuous of these splinters displaces by about 15 m 0.3-m.y.-old moat rhyolites, as well as 0.6- to 0.7-m.y.-old early rhyolites. Thus the maximum age of faulting is 0.3 m.y. However, since the intracaldera displacement about equals that on the Tioga deposits at McGee Creek, outside the caldera it probably is very much younger than 0.3 m.y. and may be in large part post-Tioga in age.

Thus both northwest and southeast of the caldera, major Sierra Nevada frontal faults having several hundred meters of postcaldera displacement show large and abrupt decreases in displacement at the caldera margins, and their intracaldera continuations apparently have been active only in very recent time. Where and how this postcaldera displacement was accommodated within the caldera is an enigma. Possibly it was accommodated on cross-caldera faults that have since been buried by younger lavas and sediments, but in the central part of the caldera where 0.6- to 0.7-m.y.-old early rhyolites are exposed, east-dipping faults with significant displacement are conspicuously absent. There is, however, some evidence of postcaldera movement on the south and southwest sectors of the caldera boundary fault. Although Pleistocene glacial deposits and steep alluvial fans have buried the actual boundary fractures on all sides of the caldera, on the south wall at Laurel and Sherwin creeks, older morainal ridges, thought to be of Mono basin age, are truncated by an apparent east-west fault

(Figure 5). Also, as noted in a preceding section, the northeast face of Mammoth Mountain, on the southwest caldera rim, is truncated by a fault that parallels the caldera wall. In contrast, the east and north walls of the caldera show no evidence of postcaldera movement on the boundary fractures. These relations suggest that during early postcaldera time, when the Long Valley magma chamber was shallow and its roof relatively thin and weak, displacement on the Sierra Nevada front between the south end of the Hartley Springs fault and the north end of the Hilton Creek fault was accommodated along the south and west sectors of the caldera boundary fault. More recently, with increased crystallization of the chamber and consequent thickening and strengthening of the roof, tectonic stresses have begun to be transmitted through the cauldron block, as indicated by the recent development of faults crossing the caldera floor on strike with the frontal faults.

This suggestion is reinforced by analysis of the deformation immediately east of the Sierra Nevada front. *Russell* [1899, p. 302] noted that the youngest shorelines of Pleistocene Mono Lake are depressed toward the range front, and *Gilbert et al.* [1968, p. 313] have described the area between Mono Lake and Long Valley as a broad, warped, faulted, grabenlike depression along the front. Southeast of Long Valley a similar depression occurs along the east base of the Wheeler Crest escarpment, where the Bishop tuff is downwarped as much as 300 m into Round Valley [*Bateman,* 1965]. Downwarping is evident also along the east and southeast rim and wall of the caldera where Pleistocene Long Valley Lake terraces are downwarped from 2320-m (7600 ft) elevation south of Glass Mountain to 2130 m (7000 ft) east of Lake Crowley (Figure 5) [*Rinehart and Ross,* 1957; *Putnam,* 1960; *Christensen,* 1966].

This zone of downwarping along the east front of the Sierra Nevada between Mono Lake and Round Valley (Figure 7*a*) constitutes a zone of backtilting or 'reverse drag' [*Hamblin,* 1965] that apparently developed simultaneously with the formation of the Sierra escarpment. A substantial amount of this downwarping postdates the caldera, but it does not appear to be continuous through the caldera (Figure 7*b*). Its continuity may be obscured partly by the resurgent dome, but the dome formed during a very short time interval immediately following caldera collapse, and any subsequent imposition of 200–300 m of downwarp should be discernible. The lack of evidence for major down-to-east faulting within and the discontinuity of 'reverse drag' across the caldera suggests that the cauldron block adjusted independently of the faulting immediately to the north and south. If postcaldera tectonic movements were restricted along the south and west sectors of the caldera boundary fault, possibly they were absorbed in the subjacent molten magma chamber, and any tendency for development of 'reverse drag' within the cauldron block was impeded by hydrostatic adjustments in the magma.

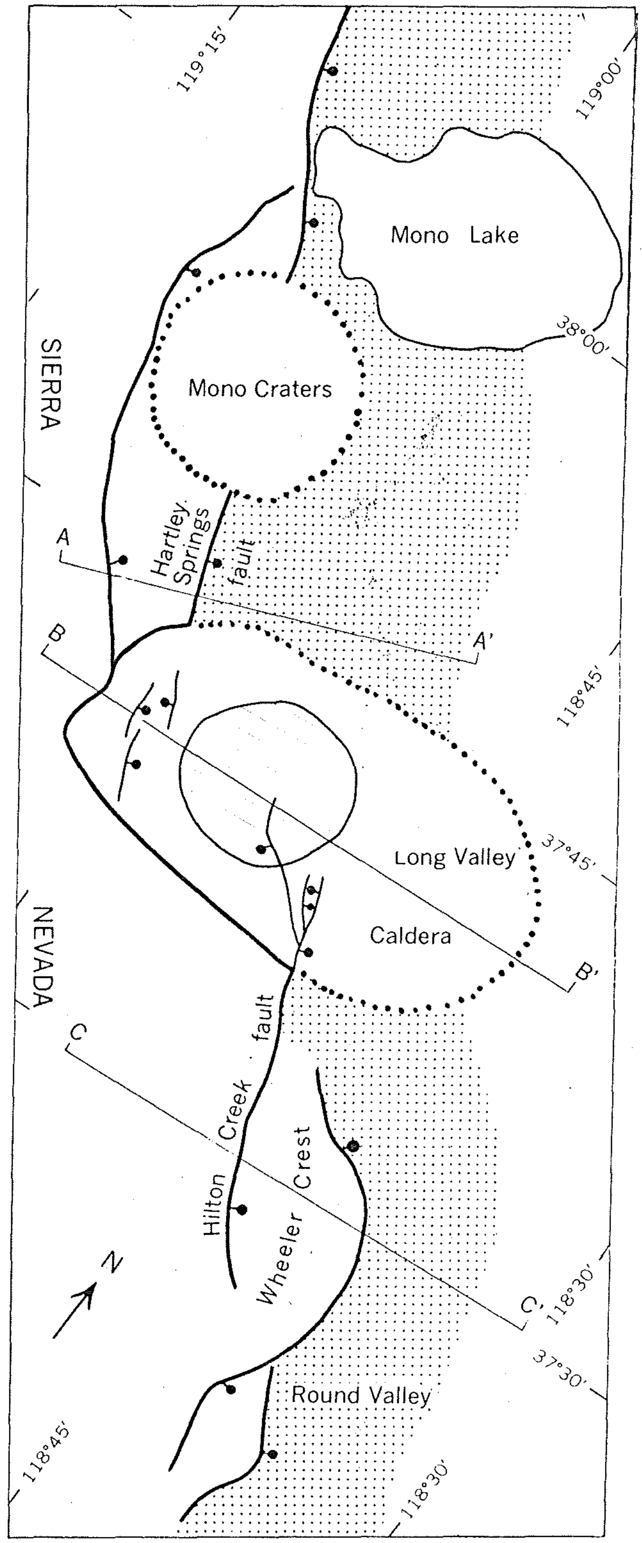

Fig. 7*a*. Tectonic map of Long Valley–Mono basin area. Heavily dotted area is zone of 'reverse drag' on Sierra Nevada front. Lined area is resurgent dome in Long Valley caldera. Solid lines represent faults (ball on downthrown side).

SUMMARY AND DISCUSSION

The structure, stratigraphy, and geochronology of Long Valley caldera are summarized in Figures 8 and 9. Volcanism in the vicinity of Long Valley began about 3.2 m.y. ago with the eruption of basalt and andesite from widely scattered centers. Subsequently, 3.0–2.7 m.y. ago, rhyodacite erupted from two main areas: the Two Teats–San Joaquin Mountain and the Bald Mountain areas, respectively west and north of Long Valley. This mafic to intermediate volcanism probably occurred during the last major rise of the Sierra Nevada and before development of the eastern Sierra Nevada escarpment. The subsequent episode of rhyolitic volcanism associated with Long Valley caldera apparently accompanied development of the escarpment, and this fundamental change in tectonic activity may have provided the conditions necessary for the generation and accumulation of large volumes of silicic magma.

Rhyolitic volcanism began about 1.9 m.y. ago northeast of

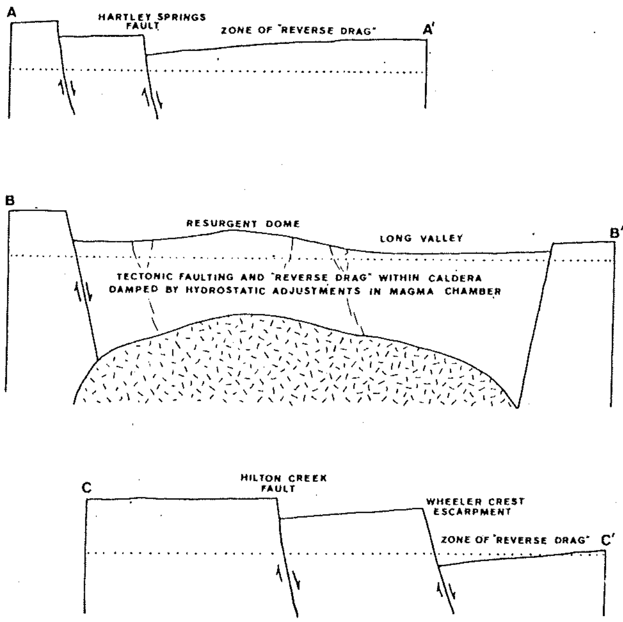

Fig. 7*b*. Schematic cross sections across the Sierra Nevada escarpment (Figure 7*a*) showing the contrast in postcaldera tectonic deformation within Long Valley caldera (BB′) and to the north (AA′) and south (CC′). Note the absence of major tectonic faults and associated 'reverse drag' within the caldera. The dotted line is an arbitrary reference level common to all three sections.

Long Valley. Sparsely porphyritic rhyolite, typically containing 77% silica, erupted over a period of 1 m.y. and accumulated in the immense edifice of Glass Mountain with its flanking pyroclastic fans. The eruptive centers of Glass Mountain are on a 13-km arcuate zone that probably coincides with an early incipient ring fracture related to development of the Long Valley magma chamber.

About 0.7 m.y. ago the Long Valley magma chamber was eviscerated by a series of explosive eruptions during which about 600 km³ of coarsely porphyritic biotite rhyolite magma containing 76% silica was ejected, mainly as ash flows, to form the Bishop tuff. Contemporaneous collapse of the roof of the chamber resulted in formation of the Long Valley caldera, an elliptical depression about 15 by 30 km and 2–3 km deep. Eruptions from at least 12 vents near the center of the caldera and possibly from others near its margins continued for 40,000–100,000 yr after collapse. During this time, at least 500 m of aphyric to sparsely porphyritic rhyolite, typically containing 75% silica, accumulated on the caldera floor. Contemporaneously with eruption of these early rhyolites the west central part of the caldera floor was uplifted into a subcircular resurgent dome about 10 km in diameter, and along its crest a 5-km-wide keystone graben formed parallel to the dominant northwest-trending precaldera structures of the region.

After resurgent doming, coarsely porphyritic hornblende-biotite rhyolite, typically containing 72% silica, erupted from three groups of centers in the caldera moat peripheral to the central resurgent dome. These three groups of moat rhyolites erupted in clockwise succession in the north, southeast, and west at 0.2-m.y. intervals about 0.5, 0.3, and 0.1 m.y. ago. About 0.2 m.y. to 50,000 yr ago, coarsely porphyritic hornblende-biotite rhyodacites containing 70–64% silica erupted on the southwest caldera rim and near the base of the northwest and north caldera walls. These rim rhyodacites constitute an outer arc of less silicic extrusions concentric with the moat rhyolites and the early rhyolites.

This concentric zonation of the postcaldera eruptives may be explained as a consequence of progressive downward crystallization of a magma chamber that was vertically zoned from rhyolite in its upper part to rhyodacite in its lower part as shown in Figure 8. The continuous decrease in silica content with time from 75% in the early rhyolites to 64% in the rim rhyodacites may be inferred to reflect intermittent tapping of the chamber at progressively greater depths along ring fractures that formed successively outward and extended downward into the congealing melt, possibly as a result of minor subsidence associated with the volume decrease that accompanied its consolidation. The upper, most silicic part of the chamber (77% silica) was erupted as the rhyolite of Glass Mountain, and during eruption of the Bishop tuff and collapse of the caldera, the chamber was drained of the zone of magma containing 76% silica. The abrupt decrease in crystal content of the magma from 20–30% in the Bishop tuff to less than 3% in the immediately subsequent early rhyolites may be the result either of phenocryst resorption caused by decompression of the chamber following eruption of the Bishop tuff or of resurgence of hotter, near-liquidus magma from deeper in the chamber. Successive tapping of deeper levels in the chamber at later times brought progressively more crystallized magma to the surface in the form of the moat rhyolites and rim rhyodacites. The simultaneous eruption of rhyolite in the west moat and rhyodacite on the rim is possibly a function of deeper consolidation on the outer edge of the magma chamber, which would require tapping of deeper, more mafic levels by outer ring fractures and of shallower, silicic levels by inner ring fractures.

Complete consolidation of a magma chamber of this type would result in a pluton zoned from granite to granodiorite downward. Documented examples of such plutons are few, the more usual zonation being concentric from more mafic to more silicic inward, but two notable examples can be cited as possible analogues: (1) the Cruachan 'granite' of the Etive and Glen Coe igneous ring complexes, Scotland, which is a binary granite on high peaks and adamellite in valley sides and floors [*Bailey and Maufe*, 1960, pp. 170, 220–221; *Anderson*, 1937], and (2) the outer 'granite' of Ben Nevis, Scotland, which in a vertical exposure of 1300 m grades from granite at high levels to granodiorite at low levels [*Anderson*, 1935, pp. 252, 264]. It is noteworthy that this latter intrusion shows the same tendency toward more coarsely porphyritic textures with apparent time as the postcaldera lavas of Long Valley.

Thermal calculations [*Lachenbruch et al.*, 1976*a*] indicate that the Long Valley magma chamber must have been replenished with heat to have sustained volcanism for more than 1 m.y.; thus the above model is probably an oversimplification. Because further refinement of it must await completion of petrochemical and mineralogical studies presently under way, discussion of the various possible mechanisms for heat replenishment seems unwarranted at this time.

During the late stages of solidification of the Long Valley chamber, basaltic and trachyandesitic lavas and pyroclastic rocks erupted from a system of north-trending fissures extending from south of the caldera through the western moat to the north shore of Mono Lake. These eruptions, possibly triggered by late faulting along the east front of the Sierra Nevada, probably tapped mafic magma from a much deeper source than the Long Valley chamber. A rare instance of the interaction of these mafic lavas with the silicic magma of the Long

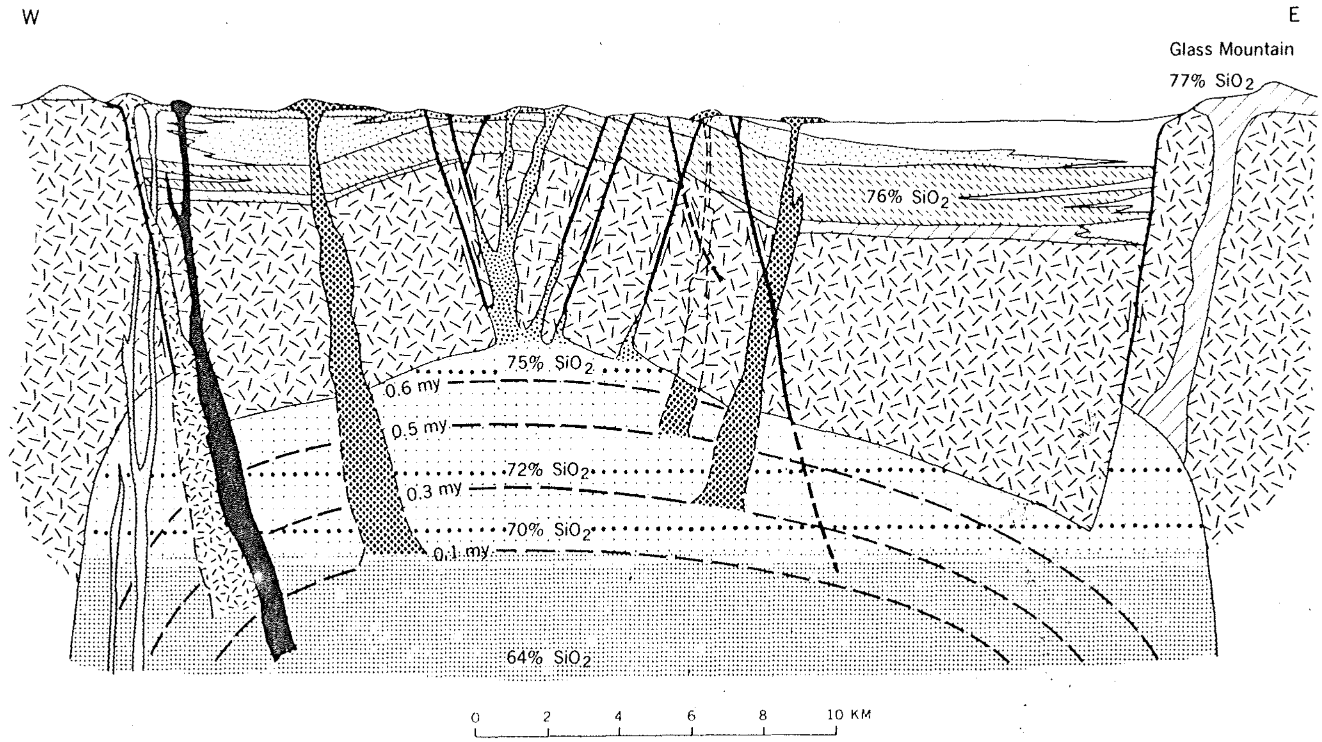

Fig. 8. Schematic east-west cross section through Long Valley caldera and its subjacent magma chamber showing hypothetical changes in chemical composition and depth of crystallization with time. The heavily dotted part of the chamber is rhyodacite magma; lightly dotted part is rhyolitic magma. Horizontal dotted lines show silica gradient in the vertically zoned chamber. Curved dashed lines show depth of crystal-liquid interface (depth to residual magma) at specified times (millions of years ago). Formation patterns are the same as in Figure 3, except that basement plutonic and metamorphic rocks (hachured) are undivided. The vertical scale is unspecified because of uncertainties in thickness of intracaldera units and depths in chamber.

Valley chamber is recorded in the mineralogically heterogeneous olivine-bearing rhyodacite of Deadman Creek.

The most recent volcanic rocks within Long Valley caldera are the Inyo domes, the youngest of which are less than 720 yr old. These domes are fluidal mixtures of rhyolitic and rhyodacitic lava that have erupted on a north-trending fissure between Long Valley caldera and the Mono craters. We interpret them as representing the mixing of rhyodacitic magma from the Long Valley chamber with rhyolitic magma from a chamber thought to underlie the Mono craters ring fracture zone. The Inyo craters, three phreatic explosion craters at the south end of the chain of Inyo domes, were possibly caused by the rise of rhyodacitic magma to very shallow depth, causing subsurface waters to flash explosively to steam. The craters may be as young as 450 yr, indicating that residual magma possibly was present in the Long Valley chamber that recently. The young age and frequency of eruptions along the Inyo-Mono volcanic chain indicate an active volcanic zone; eruptions of similar kind and magnitude could occur in the future.

Throughout most of its history, the Long Valley caldera was occupied by a lake that probably reached its highest level prior to 0.63 m.y. ago, then overflowed at the southeast rim, and subsequently was progressively lowered by tectonic faulting and warping of the rim near the outlet. Calcareous tufa deposits on the lower lake terraces indicate that in the latter part of its history the lake was alkaline and saline in composition.

Hydrothermal activity within the caldera probably reached maximum intensity about 0.3 m.y. ago. The decline of surface activity since then is probably due to 'self-sealing' of the intracaldera rocks by silicification, argillization, and zeolitization. Present thermal activity is mainly on or near recently rejuvenated segments of Sierra Nevada frontal faults that extend across the caldera and have ruptured the self-sealed cap rock. Although individual springs and fumaroles are located on or near north- to northwest-trending faults, the general distribution of hydrothermal activity is peripheral to the resurgent dome, suggesting that it is controlled at depth by the caldera ring fractures. These relations further suggest that thermal waters may be more extensive at depth than is suggested by the present surface activity.

Downfaulting on the Sierra Nevada front has continued throughout postcaldera time, but the major Sierra Nevada frontal faults that intersect the caldera rim have not displaced the caldera floor until very recently. During early postcaldera time when the magma chamber was shallow, movement on the front apparently was accommodated along the southern and western sectors of the caldera boundary fault. As the magma cooled and solidified, the cauldron block thickened and eventually became rigid enough to transmit tectonic stresses. The absence within the caldera of 'reverse drag,' present elsewhere along the Sierra Nevada front, suggests that until recently vertical tectonic stresses within the cauldron block have been absorbed by hydrostatic adjustments in the subjacent magma chamber. The manner in which the Sierra Nevada faults change from single, continuous fractures outside the caldera to branching, en echelon fractures inside suggests, however, that the cauldron block is still considerably less rigid than the surrounding crust and that it may still be partially underlain by magma.

A tentative history of the rise and consolidation of the Long Valley magma chamber can be reconstructed from several different sources of information on depth. The following esti-

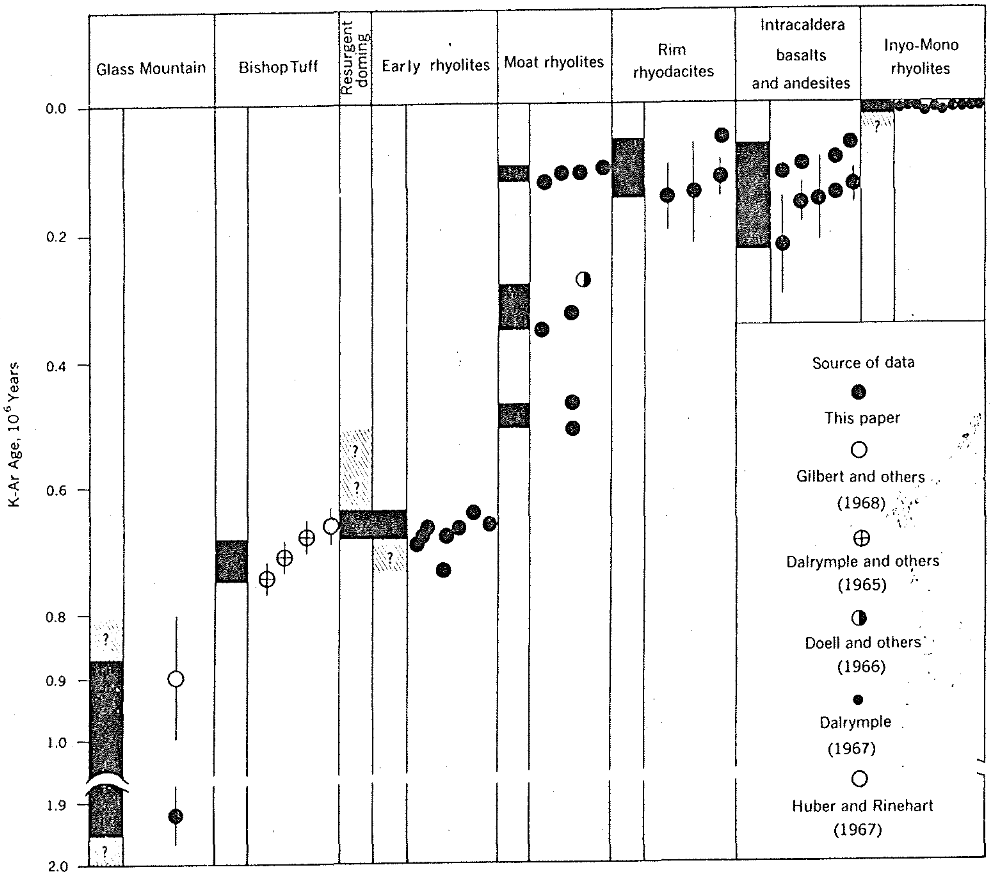

Fig. 9. K-Ar ages and inferred geochronology of volcanic events associated with Long Valley caldera. The dark bars indicate the approximate time and duration of frequent activity; lined bars with queries indicate uncertainty.

mates, although of uncertain and variable accuracy and subject to revision, are internally consistent and hence seem worth summarizing at this time. Geochemical data [*Hildreth and Spera*, 1974] suggest that at the time of eruption of the Bishop tuff 0.7 m.y. ago, the top of the chamber was at a depth of about 6 km. Structural analysis of the resurgent dome suggests that at the close of resurgence about 0.6 m.y. ago, the top of the chamber had risen to at least 5-km depth and possibly to 2 or 3 km. By about 0.2 m.y. ago the lateral encroachment of basaltic dikes on the chamber suggests that it had congealed inward and downward 4 km to a depth of 6 to possibly 9 km. Teleseismic and seismic refraction studies [*Steeples and Iyer*, 1976; *Hill*, 1976] suggest that an anomalously hot or partially molten mass still persists below 7 or 8 km. Geochemical data from the Inyo domes [*Carmichael*, 1967] indicate that lava from the Mono craters magma chamber erupted under pressures of 6.6–2.7 kbar, which suggests depths of 22–6 km.

Thus in summary, the Long Valley magma chamber appears to have developed and risen through the crust over a period of at least 1.3 m.y. (from 1.9 to 0.6 m.y. ago), during which time the rhyolites of Glass Mountain, the Bishop tuff, and the early rhyolites erupted. It then apparently achieved isostatic equilibrium in the upper crust, probably due to loss of mass. During the past 0.6 m.y. it has been cooling and congealing downward, periodically building up sufficient volatile pressure by crystallization to extrude the moat rhyolites and rim rhyodacites. Within the last 12,000 yr there has been an insurgence of new rhyolitic magma immediately to the northwest of the Long Valley chamber beneath the Mono craters, and there is some evidence in the Inyo domes that this magma has intermingled to a minor extent with the rhyodacitic residua in the Long Valley chamber.

In conclusion, volcanological, geochronological, and structural evidence indicates that large sources of heat exist at sufficiently shallow depth in the Long Valley–Mono craters area to be of importance as potential geothermal resources.

Acknowledgments. We wish to thank N. K. Huber and C. D. Rinehart for freely sharing their knowledge of the area from previous studies and for providing unpublished data and sample information that greatly facilitated the early stages of this project. We are also grateful to D. E. White for offering many helpful suggestions during the course of the fieldwork, particularly concerning the hydrothermal activity and alteration and other features associated with Pleistocene Long Valley Lake. The many exchanges of observations in the Mammoth Lakes area with S. R. Lipshie are also gratefully acknowledged. Special thanks are due to R. P. Koeppen for assistance with the mapping and sample collecting; to J. C. Von Essen, A. H. Atkinson, B. M. Myers, S. J. Kover, L. B. Schlocker, D. A. Williams, and J. Y. Saburomaru for assistance with the K-Ar analyses, and to P. C. Bateman, R. L. Christiansen, M. M. Clark, N. K. Huber, S. D. McDowell, R. P. Sharp, and D. E. White for critically reviewing the manuscript and offering many constructive suggestions.

REFERENCES

Anderson, J. G. C., The marginal intrusions of Ben Nevis, the Coille Lianachain Complex, and the Ben Nevis dyke swarm, *Trans. Geol. Soc. Glasgow*, *19*, 225–269, 1935.

Anderson, J. G. C., The Etive granite complex, 4, *Quart. J. Geol. Soc. London*, *93*, 487–533, 1937.

Bailey, E. B., and H. B. Maufe, The geology of Ben Nevis and Glen Coe and the surrounding country, *Mem. Geol. Surv. Scot.*, 1–307, 1960.

Bailey, R. A., Postsubsidence volcanism and structure of Long Valley

Caldera, California, *Geol. Soc. Amer. Abstr. Programs, 5,* 7, 1973.
Bailey, R. A., Preliminary geologic map and cross sections of the Casa Diablo geothermal area, Long Valley Caldera, Mono County, California, open file map, 2 pp., U.S. Geol. Surv., Reston, Va., 1974.
Bateman, P. C., Geology and tungsten mineralization of the Bishop district, California, *U.S. Geol. Surv. Prof. Pap. 470,* 208 pp., 1965.
Bateman, P. C., and C. Wahrhaftig, Geology of the Sierra Nevada, Geology of Northern California, *Calif. Div. Mines Geol. Bull., 190,* 107–172, 1966.
Bateman, P. C., L. D. Clark, N. K. Huber, J. G. Moore, and C. D. Rinehart, The Sierra Nevada batholith: A synthesis of recent work across the central part, *U.S. Geol. Surv. Prof. Pap. 414-D,* D1–D46, 1963.
Benioff, V. H., and B. Gutenberg, The Mammoth 'earthquake fault' and related features, *Bull. Seismol. Soc. Amer., 29,* 333–340, 1939.
Byers, F. M., Jr., P. P. Orkild, W. J. Carr, and W. D. Quinlivan, Timber Mountain tuff, southern Nevada, and its relation to cauldron subsidence, *Geol. Soc. Amer. Mem., 110,* 87–97, 1968.
Carmichael, I. S. E., The iron-titanium oxides of salic volcanic rocks and their associated ferromagnesian silicates, *Contrib. Mineral. Petrol., 14,* 36–64, 1967.
Chelikowsky, J. R., Tectonics of the rhyolite in the Mammoth embayment, California, *J. Geol., 48,* 421–435, 1940.
Christensen, M. N., Late Cenozoic crustal movements in the Sierra Nevada of California, *Geol. Soc. Amer. Bull., 77,* 163–182, 1966.
Christensen, M. N., and C. M. Gilbert, Basaltic cone suggests constructional origin of some guyots, *Science, 143,* 240–242, 1964.
Christiansen, R. L., and H. R. Blank, Volcanic evolution of the Yellowstone rhyolite plateau and eastern Snake River plain, U.S.A., in *International Association of Volcanology Symposium on Volcanoes and Their Roots,* International Association of Volcanology, Oxford, England, 1969.
Cleveland, G. B., Geology of the Little Antelope Valley clay deposits, Mono County, California, *Calif. Div. Mines Geol. Spec. Rep., 72,* 1–28, 1962.
Cox, A., and G. B. Dalrymple, Statistical analysis of geomagnetic reversal data and the precision of potassium-argon dating, *J. Geophys. Res., 72,* 2603–2614, 1967.
Curry, R. R., Glaciation about 3,000,000 years ago in the Sierra Nevada, California, *Science, 154,* 770–771, 1966.
Curry, R. R., Glacial and Pleistocene history of the Mammoth Lakes Sierra, California: A geologic guidebook, *Univ. Mont. Geol. Ser. Publ. 11,* 1–49, 1971.
Dalrymple, G. B., Potassium-argon dates of some Cenozoic volcanic rocks of the Sierra Nevada, California, *Geol. Soc. Amer. Bull., 74,* 379–390, 1963.
Dalrymple, G. B., Cenozoic chronology of the Sierra Nevada, California, *Univ. Calif. Berkeley Publ. Geol. Sci., 47,* 1–41, 1964*a*.
Dalrymple, G. B., Potassium-argon dates of three Pleistocene interglacial basalt flows from the Sierra Nevada, California, *Geol. Soc. Amer. Bull., 75,* 753–757, 1964*b*.
Dalrymple, G. B., Potassium-argon ages of Recent rhyolites of the Mono and Inyo Craters, California, *Earth Planet. Sci. Lett., 3,* 289–298, 1967.
Dalrymple, G. B., and M. A. Lanphere, *Potassium-Argon Dating,* pp. 53–85, W. H. Freeman, San Francisco, Calif., 1969.
Dalrymple, G. B., A. Cox, and R. R. Doell, Potassium-argon age and paleomagnetism of the Bishop Tuff, California, *Geol. Soc. Amer. Bull., 76,* 665–673, 1965.
Doell, R. R., G. B. Dalrymple, and A. Cox, Geomagnetic polarity epochs, Sierra Nevada data 3, *J. Geophys. Res., 71,* 531–541, 1966.
Doell, R. R., G. B. Dalrymple, R. L. Smith, and R. A. Bailey, Paleomagnetism, potassium-argon ages, and geology of rhyolites and associated rocks of the Valles Caldera, New Mexico, *Geol. Soc. Amer. Mem., 116,* 211–248, 1968.
Friedman, I., Hydration rind dates rhyolite flows, *Science, 159,* 878–880, 1968.
Friedman, I., and R. L. Smith, A new dating method using obsidian, 1, The development of the method, *Amer. Antiquity, 25,* 476–493, 1960.
Gilbert, C. M., Welded tuff in eastern California, *Geol. Soc. Amer. Bull., 49,* 1829–1862, 1938.
Gilbert, C. M., Late Tertiary geology southeast of Mono Lake, California, *Geol. Soc. Amer. Bull., 52,* 781–816, 1941.
Gilbert, C. M., M. N. Christensen, Y. Al Rawi, and K. R. Lajoie, Structural and volcanic history of Mono Basin, California-Nevada, *Geol. Soc. Amer. Mem., 116,* 275–329, 1968.
Haas, J. L., Jr., The effect of salinity on the maximum thermal gradient of a hydrothermal system at hydrostatic pressure, *Econ. Geol., 66,* 940–946, 1971.
Hamblin, W. K., Origin of 'reverse drag' on the downthrown side of normal faults, *Geol. Soc. Amer. Bull., 76,* 1145–1164, 1965.
Hildreth, W., and F. Spera, Magma chamber of the Bishop Tuff: Gradients in T, P_{total}, and $P_{\mathrm{H_2O}}$, *Geol. Soc. Amer. Abstr. Programs, 6,* 795, 1974.
Hill, D. P., Structure of Long Valley Caldera, California, from a seismic refraction experiment, *J. Geophys. Res., 81,* this issue, 1976.
Huber, N. K., and C. D. Rinehart, Geologic map of the Devils Postpile quadrangle, California, *Map GQ-437,* U.S. Geol. Surv., Reston, Va., 1965.
Huber, N. K., and C. D. Rinehart, Cenozoic volcanic rocks of the Devils Postpile quadrangle, eastern Sierra Nevada, California, *U.S. Geol. Surv. Prof. Pap. 554-D,* D1–D21, 1967.
Ingamells, C. O., Lithium metaborate flux in silicate analysis, *Anal. Chim. Acta, 52,* 323–334, 1970.
Izett, G. A., R. F. Wilcox, H. A. Powers, and G. A. Desborough, The Bishop ash bed, a Pleistocene marker bed in the western United States, *Quaternary Res., 1,* 121–132, 1970.
Jack, R. N., and I. S. E. Carmichael, The chemical 'fingerprinting' of acid volcanic rocks, *Calif. Div. Mines Geol. Spec. Rep., 100,* 17–32, 1968.
Kane, M. F., D. R. Mabey, and R.-L. Brace, A gravity and magnetic investigation of the Long Valley Caldera, Mono County, California, *J. Geophys. Res., 81,* this issue, 1976.
Keefer, W. R., The geologic story of Yellowstone National Park, *U.S. Geol. Surv. Bull., 1347,* 1–92, 1972.
Kistler, R. W., Geologic map of the Mono Craters quadrangle, Mono and Tuolumne quadrangles, California, *Map GQ-462,* U.S. Geol. Surv., Reston, Va., 1966*a*.
Kistler, R. W., Structure and metamorphism in the Mono Craters quadrangle, Sierra Nevada, California, *U.S. Geol. Surv. Bull., 1221-E,* 1–52, 1966*b*.
Lachenbruch, A. H., J. H. Sass, R. J. Monroe, and T. H. Moses, Jr., Geothermal setting and simple magmatic models for the Long Valley Caldera, *J. Geophys. Res., 81,* this issue, 1976*a*.
Lachenbruch, A. H., M. L. Sorey, R. E. Lewis, and J. H. Sass, The near-surface hydrothermal regime of Long Valley Caldera, *J. Geophys. Res., 81,* this issue, 1976*b*.
Lajoie, K. R., Late Quaternary stratigraphy and geologic history of Mono Basin, Ph.D. thesis, 271 pp., Univ. of Calif., Berkeley, 1968.
Leeman, W. P., and J. J. W. Rogers, Late Cenozoic alkali-olivine basalts of the Basin-Range province, U.S.A., *Contrib. Mineral. Petrol., 25,* 1–24, 1969.
Lipman, P. W., and T. A. Steven, Reconnaissance geology and economic significance of the Platoro Caldera, southeastern San Juan Mountains, Colorado, *U.S. Geol. Surv. Prof. Pap. 700-C,* C19–C29, 1970.
Lipman, P. W., T. A. Steven, R. G. Luedke, and W. S. Burbank, Revised volcanic history of the San Juan, Uncompahgre, Silverton, and Lake City Calderas in the western San Juan Mountains, Colorado, *U.S. Geol. Surv. J. Res., 1,* 627–642, 1973.
Mankinen, E. A., and G. B. Dalrymple, Electron microprobe evaluation of terrestrial basalts for whole-rock K-Ar dating, *Earth Planet. Sci. Lett., 17,* 89–94, 1972.
Mariner, R. H., and L. M. Willey, Geochemistry of thermal waters in Long Valley, Mono County, California, *J. Geophys. Res., 81,* this issue, 1976.
Matthes, F. E., Geography and geology of the Sierra Nevada, in *XVI International Geological Congress Guidebook,* vol. 16, part C-1, pp. 26–40, Government Printing Office, Washington, D. C., 1933.
Matthes, F. E., History of faulting movements at the east front of the Sierra Nevada, as indicated by dislocated moraines (abstract), *Geol. Soc. Amer. Bull., 50,* 1955, 1939.
Mayo, E. B., The Pleistocene Long Valley Lake in eastern California, *Science, 80,* 95–96, 1934.
Mayo, E. B., L. C. Conant, and J. R. Chelikowsky, Southern extension of the Mono Craters, California, *Amer. J. Sci., 32,* 81–97, 1936.
Muffler, L. J. P., and D. L. Williams, Geothermal investigations of the U.S. Geological Survey in Long Valley, California, *J. Geophys. Res., 81,* this issue, 1976.
Noble, D. C., M. K. Korringa, C. E. Hedge, and G. O. Riddle, Highly differentiated subalkaline rhyolite from Glass Mountain, Mono County, California, *Geol. Soc. Amer. Bull., 83,* 1179–1184, 1972.
Pakiser, L. C., Gravity, volcanism, and crustal deformation in Long Valley, California, *U.S. Geol. Surv. Prof. Pap. 424-B,* B250–B253, 1961.

Pakiser, L. C., M. F. Kane, and W. N. Jackson, Structural geology and volcanism of Owens Valley, California—A geophysical study, *U.S. Geol. Surv. Prof. Pap. 438*, 1–68, 1964.
Putnam, W. C., Quaternary geology of the June Lake district, California, *Geol. Soc. Amer. Bull., 60*, 1281–1302, 1949.
Putnam, W. C., Origin of Rock Creek and Owens River Gorges, Mono County, California, *Univ. Calif. Berkeley Publ. Geol. Sci., 34*, 221–280, 1960.
Putnam, W. C., Late Cenozoic geology of McGee Mountain, Mono County, California, *Univ. Calif. Berkeley Publ. Geol. Sci., 40*, 181–218, 1962.
Ratté, J. C., and T. A. Steven, Ash flows and related volcanic rocks associated with the Creede Caldera, San Juan Mountains, Colorado, *U.S. Geol. Surv. Prof. Pap. 524-H*, H1–H58, 1967.
Rinehart, C. D., and N. K. Huber, The Inyo Crater Lakes—A blast in the past, *Calif. Div. Mines Geol. Miner. Inform. Serv. 18*, 169–172, 1965.
Rinehart, C. D., and D. C. Ross, Geology of the Casa Diablo quadrangle, California, *Map GQ-99*, U.S. Geol. Surv., Reston, Va., 1957.
Rinehart, C. D., and D. C. Ross, Geology and mineral deposits of the Mount Morrison quadrangle, Sierra Nevada, California, *U.S. Geol. Surv. Prof. Pap. 385*, 1–106, 1964.
Russell, I. C., Quaternary history of Mono Valley, California, *Annu. Rep. 8*, pp. 261–394, U.S. Geol. Surv., Reston, Va., 1889.
Schoen, R., D. E. White, and J. J. Hemley, Argillization by descending acid at Steamboat Springs, Nevada, *Clays Clay Miner., 22*, 1–22, 1974.
Sharp, R. P., Sherwin Till-Bishop Tuff geological relationships, Sierra Nevada, California, *Geol. Soc. Amer. Bull., 79*, 351–364, 1968.
Sharp, R. P., and J. H. Birman, Additions to the classical sequence of Pleistocene glaciation, Sierra Nevada, California, *Geol. Soc. Amer. Bull., 74*, 1079–1086, 1963.
Sheridan, M. F., The mineralogy and petrology of the Bishop Tuff, Ph.D. thesis, 165 pp., Stanford Univ., Palo Alto, Calif., 1965.
Sheridan, M. F., Double cooling-unit nature of the Bishop Tuff in Owens Gorge, California (abstract), *Geol. Soc. Amer. Spec. Pap. 115*, 351, 1968.
Smith, R. L., and R. A. Bailey, Resurgent cauldrons: Their relation to granitic ring complexes and large volume ash-flow fields, in *IAV International Symposium on Volcanology*, pp. 67–68, Japan Science Council, Tokyo, 1962.
Smith, R. L., and R. A. Bailey, Resurgent cauldrons, *Geol. Soc. Amer. Mem., 116*, 613–662, 1968.
Smith, R. L., R. A. Bailey, and C. S. Ross, Structural evolution of the Valles Caldera, New Mexico, and its bearing on the emplacement of ring dikes, *U.S. Geol. Surv. Prof. Pap. 424-D*, D145–D149, 1961.
Smith, R. L., R. A. Bailey, and C. S. Ross, Geologic map of the Jemez Mountains, New Mexico, *Misc. Invest. Map I-571*, U.S. Geol. Surv., Reston, Va., 1970.
Steeples, D. W., and H. M. Iyer, Low-velocity zone under Long Valley caldera as determined from teleseismic events, *J. Geophys. Res., 81*, this issue, 1976.
Suhr, N. H., and C. O. Ingamells, Solution technique for analysis of silicates, *Anal. Chem., 38*, 730–734, 1966.
White, D. E., L. J. P. Muffler, and A. H. Truesdell, Vapor-dominated hydrothermal systems compared with hot-water systems, *Econ. Geol., 66*, 75–97, 1971.
Williams, H., and G. Goles, Volume of the Mazama ash-fall and the origin of Crater Lake caldera, *Oreg. Dep. Geol. Miner. Ind. Bull., 62*, 37–41, 1968.
Wood, S. H., Mono and Inyo Crater eruptions, eastern California—Radiocarbon dating and trace element correlations of Late Pleistocene tephra, *Geol. Soc. Amer. Abstr. Programs, 7*, 389, 1975.
U.S. Geological Survey, Geologic map of Yellowstone National Park, *Misc. Geol. Invest. Map I-711*, Reston, Va., 1972.

(Received February 20, 1975;
revised September 11, 1975;
accepted September 12, 1975.)